Hindawi
Mathematical Problems in Engineering
Volume 2019, Article ID 4687082, 20 pages
https://doi.org/10.1155/2019/4687082

Research Article

Free In-Plane Vibrations of Orthotropic Rectangular Plates by Using an Accurate Solution

Yuan Cao,[1] Rui Zhong,[2] Dong Shao,[1,3] Qingshan Wang,[2] and Dongtao Wu[3]

[1]*Naval Research Academy, Beijing 100161, China*
[2]*State Key Laboratory of High Performance Complex Manufacturing, Central South University, Changsha 410083, China*
[3]*Beijing Aerospace Technology Institute, China Aerospace Science & Industry Corp, Beijing 100074, China*

Correspondence should be addressed to Dong Shao; dongshaosatan@outlook.com

Received 29 May 2019; Revised 3 August 2019; Accepted 16 October 2019; Published 11 November 2019

Academic Editor: Arkadiusz Zak

Many numerical methods have been developed for in-plane vibration of orthotropic rectangular plates with various boundary conditions; however, the exact results for such structures with elastic boundary conditions are very scarce. Therefore, the object of this paper is to present an accurate solution for free in-plane vibration of orthotropic rectangular plates with various boundary conditions by the method of reverberation ray matrix (MRRM) and improved golden section search (IGSS) algorithm. The boundary condition studied in this paper is defined as that a set of opposite edges is with one kind of simply supported boundary conditions, while the other set is with any kind of classical and general elastic boundary conditions or their combination. Its accuracy, reliability, and efficiency are verified by some numerical examples where the results are compared with other exact solutions in the published literature and the FEA results based on the ABAQUS software. Finally, some new accurate results for free in-plane vibration of orthotropic rectangular plates with elastic boundary conditions are examined and further can be treated as the reference data for other approximate methods or accurate solutions.

1. Introduction

The orthotropic rectangular plates, as the fundamental components, have achieved a widespread use in aerospace, military, and marine industries and various engineering fields, and their structural stability and safety performance rely on the vibration characteristics. Thus, in the past decades, a lot of studies for free vibrations of rectangular plates have been carried out. Among the existing jobs, most of the researchers focus on the transverse vibrations of plates while the in-plane vibration research is very scarce. For example, Li et al. [1–4] proposed the analytical symplectic superposition method to solve free vibration solutions of rectangular plates. Zhang et al. [5, 6] presented a finite integral transform solution to determine the vibration behavior of rectangular orthotropic thin plates with different boundary conditions. Ullah et al. [7, 8] extended the integral transform method to study the buckling behavior of rectangular plates. Of course, there are many other excellent achievements, and there is no detailed discussion here. In theory, the aforementioned methods for studying transverse vibration characteristics of rectangular plates also have potential to conduct the analysis of in-plane vibration characteristics. According to the current research situation, there are relatively few related literatures on in-plane vibration characteristics of rectangular plates; the importance of which, however, has been shown in the complicated plate structures and sandwich plates [9–16]. As a matter of fact, the publications pertaining to in-plane vibrations have been increasing. In recent years, the study on in-plane vibrations has increased greatly and a lot of research results have been published.

Bardell et al. [9] studied in-plane vibrations of isotropic rectangular plates due to the lack of the related valid results at that time and provided some useful benchmark data of the in-plane frequencies of rectangular plates with simply supported, clamped, and free boundary conditions, where the Rayleigh–Ritz method is adopted. Du et al. [12] studied the in-plane vibration of isotropic rectangular plates with elastically restrained edges by the Rayleigh–Ritz method in conjunction with the Fourier series method. Gorman et al.

[17] studied in-plane vibration of rectangular plates subject to completely free boundaries by extending the superposition method. Applying the variational approximation method, Seok et al. [18] studied free in-plane vibration of a cantilevered rectangular plate. Dozio [19] studied the accurate in-plane modal properties of rectangular plates using the Ritz method, where arbitrary nonuniform elastic edge restraints were considered. Singh and Muhammad [20] investigated free in-plane vibration of isotropic nonrectangular plates subjected to classical boundary conditions using the variational method. Du et al. [21] applied a generalized Fourier method to study the free vibration of the rectangular plate with different point-supported boundary conditions, which enriched the in-plane vibration of the plate. Based on the dynamic stiffness method, Nefovska-Danilovic and Petronijevic [22] carried out the in-plane free vibration and response analysis of isotropic rectangular plates, in which the numerical results were very consistent with FEM.

In the aforementioned works, the solutions by the related solving methods like the Rayleigh–Ritz method are classified as approximate solutions. Although the methods for approximate solutions have the merits of the simple solving process and high precision, considering that the in-plane natural frequencies of plates are generally in high-frequency regions, the minor errors of results may also cause the poor structure stability and safety performance. Thus, to achieve higher precision of in-plane natural frequencies is the ultimate goal and the corresponding solution is also called the exact solution. Gorman [23] presented the exact solutions for free in-plane vibration of rectangular plates whose one set of opposite edges is simply supported and the other set both clamped or both free. Xing et al. [24, 25] obtained exact solutions for free in-plane vibrations of rectangular plates employing the direct separation of variables, where SS1-SS2-SS1-SS2, SS1-SS1-SS1-SS1, SS2-SS2-SS2-SS2, SS1-C-SS1-C, SS1-F-SS1-F, SS1-SS1-SS1-C, SS1-SS2-SS1-C, SS1-SS1-SS1-F, SS1-SS2-SS1-F, SS1-C-SS1-F, and other possible classical boundary conditions were considered. Later, Xing's [26] group obtained the exact solutions of the free in-plane vibration of orthotropic rectangular plates with SS1-C-SS1-C, SS2-F-SS2-F, SS1-C-SS2-F, SS2-SS1-SS2-C, SS2-SS2-SS2-F, and SS2-SS1-SS1-F boundary conditions. The symbols S, C, F, and E represent simply supported boundary, clamped boundary, free boundary, and elastically restrained boundary conditions, respectively. Two forms of simply supported boundary conditions are as follows [23]: SS1—displacement parallel to the edge and normal stress (N_{xx}) perpendicular to the edge are forbidden; SS2—shear stress (N_{xy}) along the edge and displacement normal to the edge are forbidden. Take boundary $x = 0$ as an example, the symbol SS1 indicates that $N_{xx} = 0$ and $v = 0$ and SS2 means that $u = 0$ and $N_{xy} = 0$.

Through the above review, it can be known that the exact solutions for in-plane vibration analysis of orthotropic rectangular plates are deficient. By investigating the existing literature, it is found that researchers have been pursuing more accurate in-plane vibration results because it can better promote the development of numerical algorithms. As far as authors know, only "*comprehensive exact solutions for free in-plane vibrations of orthotropic rectangular plates*" [26] presents the exact solutions for the titled problem. However, in this paper, only the classical boundary conditions are considered. In the existing engineering applications, there are still a large number of elastic boundaries except for the classical boundary conditions. At present, numerical methods can solve many problems well, but researchers have been pursuing the exact solution. Thus, it is necessary and urgent to establish an accurate analytical model to conduct in-plane vibration analysis of orthotropic rectangular plates with elastic boundary conditions. Before that, the members of the author's team have done some innovative work around the method of reverberation ray matrix (MRRM) in solving the exact solutions of structural vibration, such as the exact solutions of isotropic rectangular plates with elastic constraints [27]. However, it should be pointed out that the mechanical properties of orthotropic rectangular plates are superior to those of isotropic rectangular plates due to the difference of material properties. Therefore, it is necessary to study the in-plane exact solutions of orthotropic rectangular plates. This paper can be regarded as an extension of previous work.

In this paper, the method of reverberation ray matrix (MRRM) and the improved golden section search (IGSS) algorithm are adopted to solve accurate solutions for free in-plane vibration of orthotropic rectangular plates. MRRM is used to obtain the natural frequency characteristic equation and IGSS algorithm to acquire in-plane natural frequencies and modal shapes. The results are compared with existing published results and FEA results, by which the accuracy, reliability, and efficiency can be validated. On this basis, some new results for the orthotropic rectangular plates with elastic boundary conditions are presented for the first time, which may be worked as the benchmark data.

2. Theoretical Formulations of Accurate Solutions

2.1. Differential Equations and Boundary Conditions. Figure 1 shows an orthotropic rectangular plate characterized by length L_x, width L_y, and thickness h in x-, y-, and z-directions, respectively. According to the small deformation, the stresses are written as

$$\begin{aligned}\sigma_x &= A_{11}\frac{\partial u}{\partial x} + A_{12}\frac{\partial v}{\partial y},\\ \sigma_y &= A_{21}\frac{\partial u}{\partial x} + A_{22}\frac{\partial v}{\partial y},\\ \tau_{xy} &= G_{xy}\left(\frac{\partial u}{\partial y} + \frac{\partial v}{\partial x}\right),\end{aligned} \tag{1}$$

in which

$$A_{11} = \frac{E_x}{1-\mu_x\mu_y},$$

$$A_{22} = \frac{E_y}{1-\mu_x\mu_y},$$

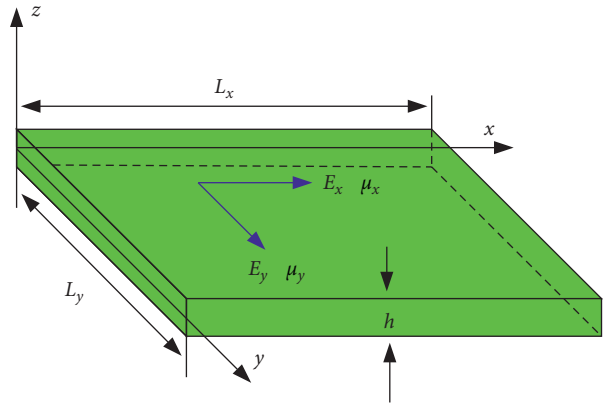

Figure 1: A rectangular plate and coordinates.

$$A_{12} = \frac{\mu_x E_y}{1 - \mu_x \mu_y},$$
$$A_{21} = \frac{\mu_y E_x}{1 - \mu_x \mu_y}, \tag{2}$$

where $E_x(E_y)$ and $\mu_x(\mu_y)$ are Young's modulus and Poisson's ratio in x-direction (y-direction), respectively, and G_{xy} is the shear modulus.

The constitutive relations of the in-plane vibration of the plate, by Hooke's law, can be expressed as

$$N_{xx} = A_{11} h \frac{\partial u}{\partial x} + A_{12} h \frac{\partial v}{\partial y},$$
$$N_{yy} = A_{21} h \frac{\partial u}{\partial x} + A_{22} h \frac{\partial v}{\partial y}, \tag{3}$$
$$N_{xy} = G_{xy} h \left(\frac{\partial u}{\partial y} + \frac{\partial v}{\partial x} \right).$$

The strain energy and kinetic energy are

$$U_V = \frac{1}{2} \int_0^{L_x} \int_0^{L_y} \left\{ N_{xx} \frac{\partial u}{\partial x} + N_{yy} \frac{\partial v}{\partial y} + N_{xy} \left(\frac{\partial u}{\partial y} + \frac{\partial v}{\partial x} \right) \right\} \mathrm{d}x\, \mathrm{d}y, \tag{4}$$

$$T = \frac{1}{2} \rho h \int_0^{L_x} \int_0^{L_y} \left\{ \frac{\partial^2 u}{\partial t^2} + \frac{\partial^2 v}{\partial t^2} \right\} \mathrm{d}x\, \mathrm{d}y, \tag{5}$$

where ρ is the mass density. As mentioned before, the aim of this study is to present an accurate solution for the free in-plane vibration of the orthotropic rectangular plate with various classical and elastic boundary conditions. Thus, to meet such requirements, the boundary simulation technique is introduced, where two opposite plate edges are implemented by the general elastic restraints (E) and other edges are simply supported restraints (S) containing the simply supported boundary 1 (SS1) and simply supported boundary 2 (SS2) to accord with the accurate solutions. The detailed information of the boundary conditions (two types: E-S-E-S and S-E-S-E) are shown as in Figure 2. Hence, the strain energy stored in these boundary springs during vibration is

$$U_S = h \int_0^{L_y} \left[k_{x0}^u u + k_{x0}^v v \right]_{x=0} dx + h \int_0^{L_y} \left[k_{x1}^u u + k_{x1}^v v \right]_{x=L_x} \mathrm{d}x, \quad \text{for E} - \text{S} - \text{E} - \text{S case},$$
$$U_S = h \int_0^{L_y} \left[k_{y0}^u u + k_{y0}^v v \right]_{y=0} dy + h \int_0^{L_y} \left[k_{y1}^u u + k_{y1}^v v \right]_{y=L_y} \mathrm{d}y, \quad \text{for S} - \text{E} - \text{S} - \text{E case}. \tag{6}$$

In the next theoretical formulations, the boundary condition is the E-S-E-S case. Within any time interval, 0 to t_0, Hamilton's principle is

$$\int_0^{t_0} (\delta U_V + \delta U_S - \delta T) \mathrm{d}t = 0, \tag{7}$$

where δU_V, δT, and δU_S are the virtual strain energy, the virtual kinetic energy, and the virtual spring potential energy, respectively, and δ is the first variation operator. Particularly, it should be pointed out here that the Hamilton's principle is a widely used principle in structural dynamics, such as linear and nonlinear vibration analysis of orthotropic or functionally graded plates.

Substituting for U_V, T, and U_S from equations (4)–(6) into equation (7) yields

$$\begin{aligned}
0 &= \int_0^{t_0} (\delta U_V + \delta U_S - \delta T) \mathrm{d}t \\
&= -\int_0^{t_0} \int_0^{L_x} \int_0^{L_y} \left\{ \frac{\partial N_{xx}}{\partial x} \delta u + \frac{\partial N_{yy}}{\partial y} \delta v + \left(\frac{\partial N_{xy}}{\partial y} \delta u + \frac{\partial N_{xy}}{\partial x} \delta v \right) \right\} \mathrm{d}x\, \mathrm{d}y\, \mathrm{d}t \\
&\quad + \int_0^{t_0} \left\{ \int_0^{L_y} \left[N_{xx} \delta u \,|_{x=0}^{x=L_x} \right] \mathrm{d}y + \int_0^{L_x} \left[N_{yy} \delta v \,|_{y=0}^{y=L_y} \right] \mathrm{d}x + \int_0^{L_x} \left[N_{xy} \delta u \,|_{y=0}^{y=L_y} \right] \mathrm{d}x + \int_0^{L_y} \left[N_{xy} \delta v \,|_{x=0}^{x=L_x} \right] \mathrm{d}y \right\} \\
&\quad + \int_0^{t_0} \left\{ \int_0^{L_y} \left[k_{x0}^u u \delta u + k_{x0}^v v \delta v \right]_{x=0} \mathrm{d}y + \int_0^{L_y} \left[k_{x1}^u u \delta u + k_{x1}^v v \delta v \right]_{x=L_x} \mathrm{d}y \right\} \mathrm{d}t \\
&\quad + \rho \int_0^{t_0} \int_0^{L_x} \int_0^{L_y} \{ \ddot{u} \delta u + \ddot{v} \delta v \} \mathrm{d}x\, \mathrm{d}y\, \mathrm{d}t.
\end{aligned} \tag{8}$$

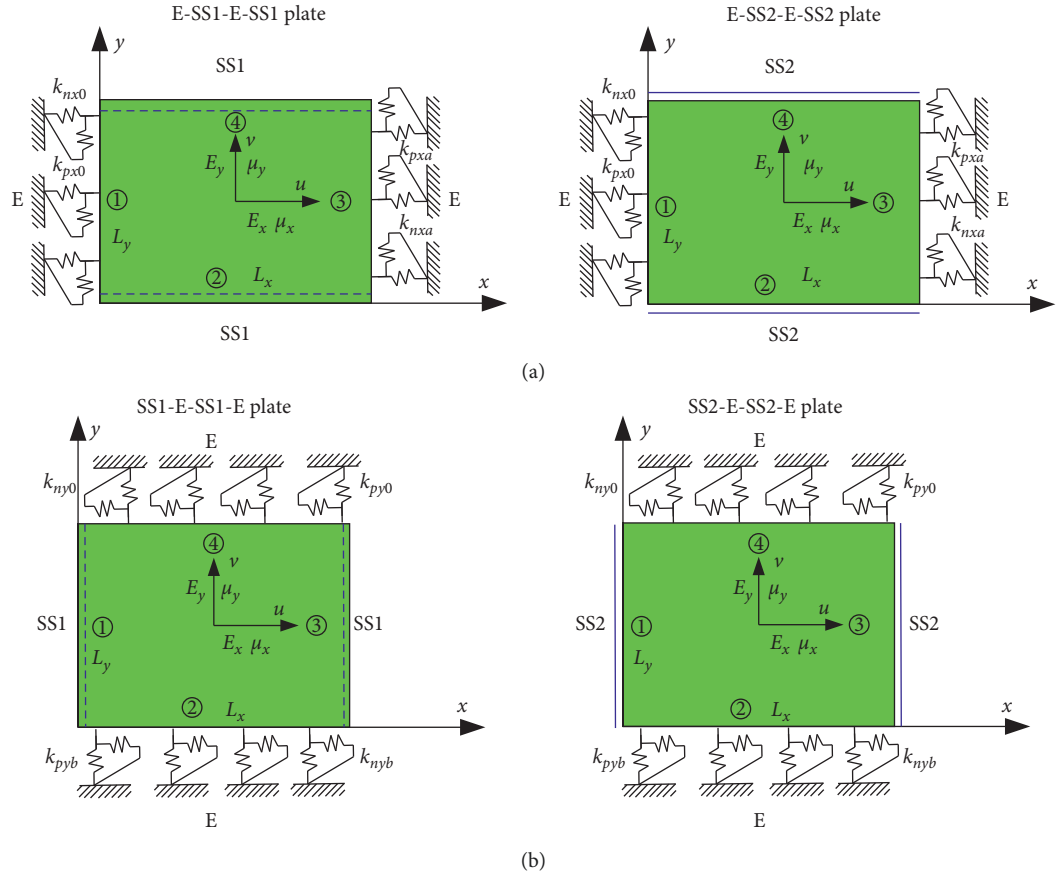

Figure 2: The four combinations of boundary conditions for free in-plane vibrations of rectangular plates with general elastic restrains along the edges: (a) x = constants and (b) y = constants.

Relieving the virtual displacements, δu and δv, in equation (8) via the integration by parts and then applying the calculus of variations yields

$$\begin{aligned} 0 = &- \int_0^{t_0}\int_0^{L_x}\int_0^{L_y}\left\{\left(\frac{\partial N_{xx}}{\partial x}+\frac{\partial N_{xy}}{\partial y}-\rho\ddot{u}\right)\delta u\right. \\ &\left.+\left(\frac{\partial N_{yy}}{\partial y}+\frac{\partial N_{xy}}{\partial x}-\rho\ddot{v}\right)\delta v\right\}\mathrm{d}x\,\mathrm{d}y\,\mathrm{d}t \\ &+\int_0^{t_0}\left\{\int_0^{L_y}\left[\left(k_{x0}^{u}u-N_{xx}\right)\delta u+\left(k_{x0}^{v}v-N_{xy}\right)\delta v\right]_{x=0}\mathrm{d}x\right. \\ &\left.+\int_0^{L_y}\left[\left(k_{xa}^{u}u+N_{xx}\right)\delta u+\left(k_{xa}^{v}v+N_{xy}\right)\delta v\right]_{x=L_x}\mathrm{d}y\right\}\mathrm{d}t. \end{aligned} \tag{9}$$

The necessary and sufficient condition for the above equation is that the virtual displacements equal to zeros because of the arbitrariness of virtual displacements. So, from the first part, the governing equations of the plate can be reduced as

$$\begin{aligned} \frac{\partial N_{xx}}{\partial x}+\frac{\partial N_{xy}}{\partial y}-\rho\ddot{u}=0, \\ \frac{\partial N_{yy}}{\partial y}+\frac{\partial N_{xy}}{\partial x}-\rho\ddot{v}=0. \end{aligned} \tag{10}$$

The elastically supported boundary conditions are expressed as

$$\begin{aligned} &\text{At } x=0, \quad k_{x0}^{u}u=N_{xx}, k_{x0}^{v}v=N_{xy}, \\ &\text{At } x=Lx, \quad k_{x1}^{u}u=-N_{xx}, k_{x1}^{v}v=-N_{xy}. \end{aligned} \tag{11a}$$

In the same way, the elastically supported condition for S-E-S-E case (Figure 2(b)) can also be obtained as follows:

$$\begin{aligned} &\text{At } y=0, \quad k_{y0}^{u}u=N_{xy}, k_{y0}^{v}v=N_{yy}, \\ &\text{At } y=Ly, \quad k_{y1}^{u}u=-N_{xy}, k_{y1}^{v}v=-N_{yy}. \end{aligned} \tag{11b}$$

2.2. Wave Solutions. In Section 2.1, the derivations are in the time domain. But, the free in-plane vibration analysis is in the frequency domain. Therefore, the Laplace transform is primarily applied to obtain the corresponding differential equations and boundary equations in the frequency domain. The expressions of Laplace transform and inverse Laplace transform are

$$\begin{aligned} \hat{\mathbf{v}}(x,y,s)&=\int_0^{\infty}\mathbf{v}(x,y,t)e^{-st}\mathrm{d}t, \\ \mathbf{v}(x,y,t)&=\frac{1}{2\pi i}\int_{\beta-\infty i}^{\beta+\infty i}\hat{\mathbf{v}}(x,y,s)e^{st}\mathrm{d}s, \end{aligned} \tag{12}$$

where β is the intersection point between the Bromwich contour of integration and the real axis on the complex s-plane.

The in-plane governing equations in equation (10) can be rewritten as the following form by the Laplace transform:

$$\begin{bmatrix} L_{11} & L_{12} \\ L_{12} & L_{22} \end{bmatrix} \begin{bmatrix} \widehat{u} \\ \widehat{v} \end{bmatrix} = \begin{bmatrix} \rho s^2 & 0 \\ 0 & \rho s^2 \end{bmatrix} \begin{bmatrix} \widehat{u} \\ \widehat{v} \end{bmatrix}, \tag{13}$$

where the coefficients of the linear operator L ($L_{ij} = L_{ji}$) are given as follows:

$$\begin{aligned} L_{11} &= A_{11}\frac{\partial^2}{\partial x^2} + G_{xy}\frac{\partial^2}{\partial y^2}, \\ L_{12} &= A_{12}\frac{\partial^2}{\partial x\,\partial y} + G_{xy}\frac{\partial^2}{\partial x\,\partial y}, \\ L_{22} &= A_{22}\frac{\partial^2}{\partial y^2} + G_{xy}\frac{\partial^2}{\partial x^2}. \end{aligned} \tag{14}$$

The accurate forms of generalized displacement functions for in-plane vibration of the orthotropic rectangular plate whose edges of $y = 0$ and $y = L_y$ are with classical boundary conditions are

$$\begin{aligned} \widehat{u}(x, y) &= \sum_{n=1}^{\infty} A_n e^{\lambda_n x} U_{yn}(y), \\ \widehat{v}(x, y) &= \sum_{n=1}^{\infty} B_n e^{\lambda_n x} V_{yn}(y), \end{aligned} \tag{15}$$

where A_n and B_n, the arbitrary coefficients, correspond to the generalized displacement amplitudes for the nth mode of the plate, λ_n is the characteristic wave number in the x-direction, and $U_{yn}(y)$ and $V_{yn}(y)$ are in-plane modal functions for the plate whose y-direction is with different boundaries; and for the case of two parallel edges $y = 0$ and $y = L_y$ with the simply supported boundary, their expressions are written as

$$\begin{aligned} &\text{SS1: } U_{yn}(y) = \sin\left(k_y y\right), V_{yn}(y) = \cos\left(k_y y\right), \quad \left(k_y = \frac{n\pi}{L_y}\right), \\ &\text{SS2: } U_{yn}(y) = \cos\left(k_y y\right), V_{yn}(y) = \sin\left(k_y y\right), \quad \left(k_y = \frac{n\pi}{L_y}\right). \end{aligned} \tag{16}$$

Then, substituting the above wave solutions into equation (12), two homogeneous linear equations are obtained, which can be also written in the following matrix form:

$$\begin{bmatrix} T_{11} & T_{12} \\ T_{21} & T_{22} \end{bmatrix} \begin{bmatrix} U_n \\ V_n \end{bmatrix} = |\mathbf{T}|\mathbf{C}_n = 0, \tag{17}$$

where the elements of T_{ij} ($i, j = 1,2$) are

SS1:

$$\begin{aligned} T_{11} &= -G_{xy}k_y^2 + A_{11}\lambda_n^2 - \rho s^2, \\ T_{12} &= -k_y\lambda_n\left(G_{xy} + A_{12}\right), \\ T_{21} &= k_y\lambda_n\left(G_{xy} + A_{12}\right), \\ T_{22} &= -A_{22}k_y^2 + G_{xy}\lambda_n^2 - \rho s^2. \end{aligned}$$

SS2:

$$\begin{aligned} T_{11} &= -G_{xy}k_y^2 + A_{11}\lambda_n^2 - \rho s^2, \\ T_{12} &= k_y\lambda_n\left(G_{xy} + A_{12}\right), \\ T_{12} &= k_y\lambda_n\left(G_{xy} + A_{12}\right), \\ T_{22} &= -A_{22}k_y^2 + G_{xy}\lambda_n^2 - \rho s^2. \end{aligned} \tag{18}$$

For equation (17), if and only if the determinant of the coefficient matrix equals to zero, its nontrivial solutions can be obtained and the characteristic equation of λ_n is

$$b_4\lambda_n^4 + b_2\lambda_n^2 + b_0 = 0, \tag{19}$$

where

$$\begin{aligned} b_0 &= \rho^2 s^4 + A_{22}G_{xy}k_y^4 + A_{22}k_y^2\rho s^2 + G_{xy}k_y^2\rho s^2, \\ b_2 &= A_{12}^2k_y^2 - A_{11}A_{22}k_y^2 + 2A_{12}G_{xy}k_y^2 - A_{11}\rho s^2 - G_{xy}\rho s^2, \\ b_4 &= A_{11}G_{xy}. \end{aligned} \tag{20}$$

For equation (19), when the wave number is zero, the rigid-body displacements occur, but in free vibration, such displacements will be eliminated. By solving equation (19), two pairs of characteristic wave numbers $\pm\lambda_{1n}$ and $\pm\lambda_{2n}$ can be obtained, and the corresponding basic solution vectors of equation (17), $\{\alpha_{a,din}, 1\}^T$ ($i = 1, 2$), are defined by

$$\begin{aligned} \alpha_{a,d1n} &= -\left.\frac{T_{12}}{T_{11}}\right|_{\lambda=\pm\lambda_{1n}}, \\ \alpha_{a,d2n} &= -\left.\frac{T_{12}}{T_{11}}\right|_{\lambda=\pm\lambda_{2n}}. \end{aligned} \tag{21}$$

Then, the general solutions for the orthotropic rectangular plate displacements are obtained by the superposition principle:

$$\begin{aligned} u(x, y) &= \sum_{n=1}^{\infty}\left\{a_{1n}e^{\lambda_{1n}x} + a_{2n}e^{\lambda_{2n}x} + d_{1n}e^{-\lambda_{1n}x} + d_{2n}e^{-\lambda_{2n}x}\right\}U_{yn}(y), \\ v(x, y) &= \sum_{n=1}^{\infty}\left\{\alpha_{a1n}a_{1n}e^{\lambda_{1n}x} + \alpha_{a2n}a_{2n}e^{\lambda_{2n}x} + \alpha_{d1n}d_{1n}e^{-\lambda_{1n}x}\right. \\ &\quad \left. + \alpha_{d2n}d_{2n}e^{-\lambda_{2n}x}\right\}V_{yn}(y). \end{aligned} \tag{22}$$

To apply the MRRM further, a generalized displacement vector $\widehat{\boldsymbol{\delta}}$ is introduced:

$$\boldsymbol{\delta}_{\mathbf{n}} = \mathbf{Y}_{\mathbf{n}}(y)\mathbf{A}_{\mathbf{n}\boldsymbol{\delta}}\mathbf{P}_{\mathbf{n}}(-x)\mathbf{a}_{\mathbf{n}} + \mathbf{Y}_{\mathbf{n}}(y)\mathbf{D}_{\mathbf{n}\boldsymbol{\delta}}\mathbf{P}_{\mathbf{n}}(x)\mathbf{d}_{\mathbf{n}}, \tag{23}$$

where

$$\begin{aligned}
\mathbf{Y_n} &= \operatorname{diag}\left(U_{yn}(y), V_{yn}(y)\right),\\
\mathbf{P_n}(x) &= \operatorname{diag}\left(e^{-\lambda_{1n}x}, e^{-\lambda_{2n}x}\right),\\
\mathbf{a_n} &= \left[\, a_{1n} \;\; a_{2n} \,\right]^T,\\
\mathbf{d_n} &= \left[\, d_{1n} \;\; d_{2n} \,\right]^T,\\
\mathbf{A_{n\delta}} &= \begin{bmatrix} 1 & 1 \\ \alpha_{a1n} & \alpha_{a2n} \end{bmatrix},\\
\mathbf{D_{n\delta}} &= \begin{bmatrix} 1 & 1 \\ \alpha_{d1n} & \alpha_{d2n} \end{bmatrix},
\end{aligned} \tag{24}$$

where $\mathbf{P_n}(x)$ is the phase propagation matrix and $\mathbf{A_{n\delta}}$ and $\mathbf{D_{n\delta}}$ are the displacement coefficient matrixes. The boundary forces, similarly, can be written as a generalized displacement vector $\mathbf{f_n}$:

$$\mathbf{f_n} = \left[N_{xx}, N_{xy}\right]^T = \mathbf{Y_n}(y)\mathbf{A_{nf}}\mathbf{P_n}(-x)\mathbf{a_n} + \mathbf{Y_n}(y)\mathbf{D_{nf}}\mathbf{P_n}(x)\mathbf{d_n}, \tag{25}$$

where

$$\text{SS1:}\begin{cases}
\mathbf{A_{nf}} = \begin{bmatrix} A_{11}\lambda_{1n} - A_{12}\alpha_{a1n}k_y & A_{11}\lambda_{2n} - A_{12}\alpha_{a2n}k_y \\ G_{xy}\left(\alpha_{a1n}\lambda_{1n} + k_y\right) & G_{xy}\left(\alpha_{a2n}\lambda_{2n} + k_y\right) \end{bmatrix},\\
\mathbf{D_{nf}} = \begin{bmatrix} -A_{11}\lambda_{1n} - A_{12}\alpha_{d1n}k_y & -A_{11}\lambda_{2n} - A_{12}\alpha_{d2n}k_y \\ G_{xy}\left(k_y - \alpha_{d1n}\lambda_{1n}\right) & G_{xy}\left(k_y - \alpha_{d2n}\lambda_{2n}\right) \end{bmatrix},
\end{cases}$$

$$\text{SS2:}\begin{cases}
\mathbf{A_{nf}} = \begin{bmatrix} A_{11}\lambda_{1n} + A_{12}\alpha_{a1n}k_y & A_{11}\lambda_{2n} + A_{12}\alpha_{a2n}k_y \\ G_{xy}\left(\alpha_{a1n}\lambda_{1n} - k_y\right) & G_{xy}\left(\alpha_{a2n}\lambda_{2n} - k_y\right) \end{bmatrix},\\
\mathbf{D_{nf}} = \begin{bmatrix} -A_{11}\lambda_{1n} + A_{12}\alpha_{d1n}k_y & -A_{11}\lambda_{2n} + A_{12}\alpha_{d2n}k_y \\ G_{xy}\left(-k_y - \alpha_{d1n}\lambda_{1n}\right) & G_{xy}\left(-k_y - \alpha_{d2n}\lambda_{2n}\right) \end{bmatrix}.
\end{cases} \tag{26}$$

2.3. Accurate Solutions for Free In-Plane Vibration of Rectangular Plates. The artificial spring boundary technique and the method of reverberation ray matrix are used together to derive the reverberation ray matrix approach in this section and then to conduct the analysis of in-plane vibration for orthotropic rectangular plates with general boundary conditions [28–33].

In the orthotropic rectangular plates, the dual local coordinates (o-$x^{12}y^{12}z^{12}$) and (o-$x^{21}y^{21}z^{21}$) should be established to determine the phase relation of the reverberation ray groups. For information on double local coordinates, please refer to reference [27]. The origins of the two dual local coordinates, nodes "1" and "2," are set at the right and left edges of the plate. For brevity, it is assumed that (o-$x^{12}y^{12}z^{12}$) and (o-$x^{21}y^{21}z^{21}$) are both paralleled with the global coordinate (o-xyz) but their x- and z-coordinates are in the opposite directions, and dual local coordinates satisfy the following relation:

$$\begin{aligned}
x^{12} &= L_x - x^{21},\\
y^{12} &= y^{21},\\
z^{12} &= -z^{21}.
\end{aligned} \tag{27}$$

In the dual local coordinate systems, the generalized state vectors $\boldsymbol{\delta}_\mathbf{n}$ and $\mathbf{f_n}$ in equations (23) and (25) are written as

$$\begin{Bmatrix} \boldsymbol{\delta}^{12}\left(x^{12}\right) \\ \mathbf{f}^{12}\left(x^{12}\right) \end{Bmatrix} = \begin{bmatrix} \mathbf{A}^{12}_{n\delta}\mathbf{P}\left(-x^{12}\right) & \mathbf{D}^{12}_{n\delta}\mathbf{P}\left(x^{12}\right) \\ \mathbf{A}^{12}_{nf}\mathbf{P}\left(-x^{12}\right) & \mathbf{D}^{12}_{nf}\mathbf{P}\left(x^{12}\right) \end{bmatrix} \begin{Bmatrix} \mathbf{a}^{12}_\mathbf{n} \\ \mathbf{d}^{12}_\mathbf{n} \end{Bmatrix}, \tag{28}$$

$$\begin{Bmatrix} \boldsymbol{\delta}^{21}\left(x^{21}\right) \\ \mathbf{f}^{21}\left(x^{21}\right) \end{Bmatrix} = \begin{bmatrix} \mathbf{A}^{21}_{n\delta}\mathbf{P}\left(-x^{21}\right) & \mathbf{D}^{21}_{n\delta}\mathbf{P}\left(x^{21}\right) \\ \mathbf{A}^{21}_{nf}\mathbf{P}\left(-x^{21}\right) & \mathbf{D}^{21}_{nf}\mathbf{P}\left(x^{21}\right) \end{bmatrix} \begin{Bmatrix} \mathbf{a}^{21}_\mathbf{n} \\ \mathbf{d}^{21}_\mathbf{n} \end{Bmatrix}. \tag{29}$$

Furthermore, because of the uniqueness of the physical quantity, the compatibility condition of generalized state variables can be determined on the basis of the sign convention (seen in Figure 3):

$$\begin{aligned}
\left[u_0^{12}, v_0^{12}\right] &= \left[-u_0^{21}, v_0^{21}\right],\\
\boldsymbol{\delta}^{12}\left(x^{12}\right) &= \mathbf{T}_\delta\boldsymbol{\delta}^{21}\left(x^{21}\right),
\end{aligned} \tag{30a}$$

$$\begin{aligned}
\left[N_{xx}^{12}, N_{xy}^{12}\right] &= \left[N_{xx}^{21}, -N_{xy}^{21}\right],\\
\mathbf{f}_n^{12}\left(x^{12}\right) &= \mathbf{T}_f\mathbf{f}_n^{21}\left(x^{21}\right),
\end{aligned} \tag{30b}$$

where $\mathbf{T}_\delta = \operatorname{diag}\{-1, 1\}$ is the dual transformation matrix between $\boldsymbol{\delta}^{12}$ and $\boldsymbol{\delta}^{21}$ and $\mathbf{T}_f = \operatorname{diag}\{1, -1\}$ that between $\mathbf{f}^{12}$ and $\mathbf{f}^{21}$. Substituting equations (27)–(29) into equations (30a) and (30b) and considering the wave numbers are independent of two dual local coordinates, i.e., $\lambda_i^{12} = \lambda_i^{21}$ ($i = 1, 2$), we have

$$\begin{bmatrix} \mathbf{A_{n\delta}}\mathbf{P_n}(0) & \mathbf{D_{n\delta}}\mathbf{P_n}(0) \\ \mathbf{A_{nf}}\mathbf{P_n}(0) & \mathbf{D_{nf}}\mathbf{P_n}(0) \end{bmatrix} \begin{bmatrix} \mathbf{a}^{21}_\mathbf{n} \\ \mathbf{d}^{21}_\mathbf{n} \end{bmatrix} = \begin{bmatrix} \mathbf{T}_\delta & 0 \\ 0 & \mathbf{T}_\mathbf{f} \end{bmatrix} \begin{bmatrix} \mathbf{A_{n\delta}}\mathbf{P_n}\left(-L_x\right) & \mathbf{D_{n\delta}}\mathbf{P_n}\left(L_x\right) \\ \mathbf{A_{nf}}\mathbf{P_n}\left(-L_x\right) & \mathbf{D_{nf}}\mathbf{P_n}\left(L_x\right) \end{bmatrix} \begin{bmatrix} \mathbf{a}^{12}_\mathbf{n} \\ \mathbf{d}^{12}_\mathbf{n} \end{bmatrix}, \tag{31}$$

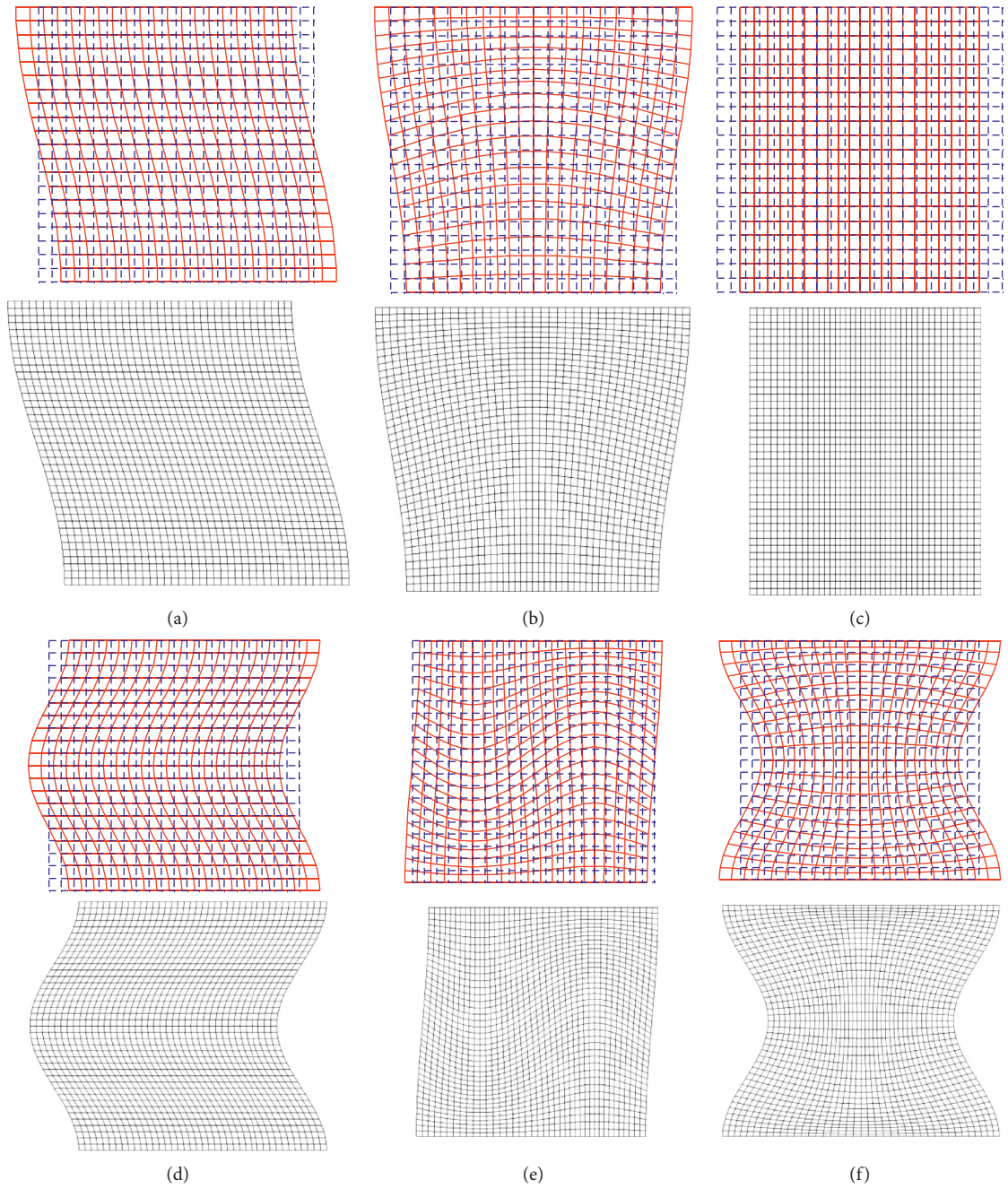

Figure 3: The mode shapes of the SS1-SS2-SS1-SS2 plate (red line: present solution; black line: ABAQUS software). (a) 1st mode. (b) 2nd mode. (c) 3rd mode. (d) 4th mode. (e) 5th mode. (f) 6th mode.

which can be regrouped as

$$\begin{bmatrix} -\mathbf{T}_{\delta}\mathbf{A}_{n\delta}\mathbf{P}_{n}(-L_x) & \mathbf{A}_{n\delta}\mathbf{P}_{n}(0) \\ -\mathbf{T}_{f}\mathbf{A}_{nf}\mathbf{P}_{n}(-L_x) & \mathbf{A}_{nf}\mathbf{P}_{n}(0) \end{bmatrix} \begin{bmatrix} \mathbf{a}_{n}^{12} \\ \mathbf{a}_{n}^{21} \end{bmatrix} = \begin{bmatrix} \mathbf{T}_{\delta}\mathbf{D}_{n\delta}\mathbf{P}_{n}(L_x) & -\mathbf{D}_{n\delta}\mathbf{P}_{n}(0) \\ \mathbf{T}_{f}\mathbf{D}_{nf}\mathbf{P}_{n}(L_x) & -\mathbf{D}_{nf}\mathbf{P}_{n}(0) \end{bmatrix} \begin{bmatrix} \mathbf{d}_{n}^{12} \\ \mathbf{d}_{n}^{21} \end{bmatrix}. \tag{32}$$

Also, equation (32) can be further simplified as

$$\overline{\mathbf{a}} = \mathbf{P}_{h}\overline{\mathbf{d}}, \tag{33}$$

where $\overline{\mathbf{a}} = \left\{[\mathbf{a}_{n}^{12}]^{T}, [\mathbf{a}_{n}^{21}]^{T}\right\}^{T}$ and $\overline{\mathbf{d}} = \left\{[\mathbf{d}_{n}^{12}]^{T}, [\mathbf{d}_{n}^{21}]^{T}\right\}^{T}$ are the wave amplitude vectors and

$$\mathbf{P}_h = \begin{bmatrix} -\mathbf{T}_\delta \mathbf{A}_{n\delta} \mathbf{P}_n(-L_x) & \mathbf{A}_{n\delta} \mathbf{P}_n(0) \\ -\mathbf{T}_f \mathbf{A}_{nf} \mathbf{P}_n(-L_x) & \mathbf{A}_{nf} \mathbf{P}_n(0) \end{bmatrix}^{-1} \begin{bmatrix} \mathbf{T}_\delta \mathbf{D}_{n\delta} \mathbf{P}_n(L_x) & -\mathbf{D}_{n\delta} \mathbf{P}_n(0) \\ \mathbf{T}_f \mathbf{D}_{nf} \mathbf{P}_n(L_x) & -\mathbf{D}_{nf} \mathbf{P}_n(0) \end{bmatrix}, \tag{34}$$

is the phase matrix expressing the phase relations of wave amplitude vectors. To ensure numerical stability of calculation, the exponentially growing function should not occur in the phase matrix, which indicates that the wave numbers λ_i $(i = 1, 2)$ should have the positive real part.

Next, the system wave amplitude vectors are completely determined by the scattering relations at each of the nodes. According to the boundary conditions given in equations (11a) and (11b), the displacement continuity and force equilibrium conditions of the node are written as

$$\mathbf{A}_{nf}^{12} \mathbf{a}_n^{12} + \mathbf{D}_{nf}^{12} \mathbf{d}_n^{12} = \mathbf{K}_E^1 \left(\mathbf{A}_{n\delta}^{12} \mathbf{a}_n^{12} + \mathbf{D}_{n\delta}^{12} \mathbf{d}_n^{12} \right), \tag{35}$$

$$\mathbf{A}_{nf}^{21} \mathbf{a}_n^{21} + \mathbf{D}_{nf}^{21} \mathbf{d}_n^{21} = \mathbf{K}_E^2 \left(\mathbf{A}_{n\delta}^{21} \mathbf{a}_n^{21} + \mathbf{D}_{n\delta}^{21} \mathbf{d}_n^{21} \right), \tag{36}$$

where $\mathbf{K}_E^1 = \mathrm{diag}\{k_{x0}^u, k_{x0}^v\}$ and $\mathbf{K}_E^2 = \mathrm{diag}\{k_{x1}^u, k_{x1}^v\}$ are stiffness matrices of the two sets of support springs. By changing the stiffness values, all possible boundary conditions can be simulated. Here, the boundary stiffness matrixes shown in Table 1 correspond to several boundary conditions often encountered in practice. Then, by classifications and reorganizations further, equations (33) and (34) are expressed in the following form of matrix:

$$\overline{\mathbf{d}} = \mathbf{S}\overline{\mathbf{a}}, \tag{37}$$

where

$$\mathbf{S} = \begin{bmatrix} \left(\mathbf{K}_E^1 \mathbf{D}_{n\delta}^{12} - \mathbf{D}_{nf}^{12} \right)^{-1} \left(\mathbf{A}_{nf}^{12} - \mathbf{K}_E^1 \mathbf{A}_{n\delta}^{12} \right) & 0 \\ 0 & \left(\mathbf{K}_E^2 \mathbf{D}_{n\delta}^{21} - \mathbf{D}_{nf}^{21} \right)^{-1} \left(\mathbf{A}_{nf}^{21} - \mathbf{K}_E^2 \mathbf{A}_{n\delta}^{21} \right) \end{bmatrix}, \tag{38}$$

is the scattering matrix. Further combining equations (33) and (37) yields

$$(\mathbf{I} - \mathbf{R})\overline{d} = \mathbf{0}, \tag{39}$$

where $\mathbf{R} = \mathbf{S}\mathbf{P}_h$ is the reverberation ray matrix.

The equation of natural frequencies for free vibration is expressed as

$$\det(\mathbf{I} - \mathbf{R}) = \mathbf{0}. \tag{40}$$

For equation (40), it can be known that it is transcendental, which brings difficulty in solving analytically. Thus, an effective search technique is established by the author's group based on the extrapolation method and golden section search (GSS) algorithm to obtain nontrivial solutions of equation (40). The detailed principle of the effective search technique can be seen in reference [27, 34].

3. Numerical Results and Discussion

Section 2 shows the theoretical formulations of the present accurate solutions. Thus, in this section, the primary purpose is to verify its accuracy and reliability via several numerical examples including the comparison of in-plane frequency parameters and modal shapes. On the basis of that some new in-plane vibration results of orthotropic rectangular plates with elastic boundary condition are presented.

Tables 2–5 show the first ten in-plane frequency parameters of orthotropic rectangular plates with different classical boundary conditions. In Tables 2–4, the finite element method (FEM) results taken from the ABAQUS software are also given as comparison due to the lack of the accurate benchmark data. In the FEM results, two types of the modeling methods are considered: FEMI: mesh size 0.025 m × 0.025 m, mesh type: S4R, and mesh number: 1600; FEMII: mesh size 0.01 m × 0.01 m, mesh type: S4R, and mesh number: 10000. In addition, the corresponding in-plane modal shapes of Tables 2–4 are presented in Figures 3–5, respectively. In Table 5, the results by Du et al. [12] using a semianalytical method and Liu and Xing [26] using the exact solutions are also considered here. In Tables 2–5, the dimensionless formula Ω is defined as $\omega L_x(\rho/G_{xy})^{1/2}/\pi$, and the geometric parameters and material parameters are given as follows: $L_x/L_y = 1$, $\mu_x = 0.3$, $E_y = 70$ GPa, $E_x = 2E_y$, and $G_{xy} = E_y/2/(1 - \mu_x\mu_y)$. From Tables 2–5, it is obvious that the results of present accurate solutions are close to the referential solutions. In addition, it is also clear from Tables 2–4 that the accuracy of the finite element method depends strongly on the mesh type and size of the finite element model. In theory, the smaller the size of the element, the more the number of the element, and the higher the accuracy of the calculation at this time; however, more computing resources need to be paid. This is why the purpose of developing exact solutions is to provide reference for numerical solutions [3, 4].

From Tables 2–5, it can also be concluded that the present approach has good accuracy and reliability in the analysis of in-plane vibration of orthotropic rectangular plates. However, in Section 1, it can be known that although relevant research has been carried out in the study of isotropic rectangular plates [27], no parametric study of the exact elastic solutions for the orthogonal materials has been found. Therefore, in order to enrich the existing research system and results, some parametric research work on elastic

Table 1: Essential conditions and stiffness matrixes for different boundary conditions.

Boundary conditions	Corresponding stiffness matrixes (N/m)	Essential conditions
Free (F)	$\mathrm{diag}(0, 0)$	$N_{xx} = N_{xy} = 0$
Clamped (C)	$\mathrm{diag}(10^{18}, 10^{18})$	$u = v = 0$
Simply supported 1 (SS1)	$\mathrm{diag}(0, 10^{18})$	$N_{xx} = 0,\ v = 0$
Simply supported 2 (SS2)	$\mathrm{diag}(10^{18}, 0)$	$u = 0,\ N_{xy} = 0$
Elastic restrained (E)	$\mathrm{diag}(k^u_{x0(x1)}, k^v_{x0(x1)})$	$u = v \neq 0$

Table 2: Comparison of the in-plane frequency parameters Ω for E-SS1-E-SS1 orthotropic rectangular plates.

B.C	Method	Mode sequence									
		1	2	3	4	5	6	7	8	9	10
C-SS1-SS1-SS1	FEMI	1.0025	1.2700	1.7631	2.0199	2.1365	2.2958	2.6993	3.0669	3.1315	3.1358
	FEMII	1.0005	1.2684	1.7611	2.0044	2.1230	2.2834	2.6888	3.0148	3.0872	3.1205
	Present	1.0000	1.2679	1.7605	2.0000	2.1192	2.2800	2.6860	3.0000	3.0735	3.1176
C-SS1-C-SS1	FEMI	1.0025	1.6926	2.0026	2.0199	2.5527	2.6157	2.8675	3.0669	3.2100	3.3917
	FEMII	1.0005	1.6908	1.9961	2.0044	2.5395	2.6063	2.8603	3.0148	3.1651	3.3489
	Present	1.0000	1.6904	1.9942	2.0000	2.5358	2.6037	2.8586	3.0000	3.1524	3.3368
SS1-SS1-SS1-SS1	FEMI	1.0025	1.0025	1.4558	2.0199	2.0199	2.2834	2.3060	2.4283	2.9243	3.0669
	FEMII	1.0005	1.0005	1.4541	2.0044	2.0044	2.2701	2.2963	2.4266	2.9109	3.0148
	Present	1.0000	1.0000	1.4537	2.0000	2.0000	2.2664	2.2937	2.4263	2.9074	3.0000
SS1-SS1-F-SS1	FEMI	0.5003	0.8460	1.4186	1.5081	1.7975	1.8223	2.2665	2.3757	2.5373	2.7962
	FEMII	0.5001	0.8437	1.4174	1.5018	1.7942	1.8056	2.2559	2.3689	2.5084	2.7421
	Present	0.5000	0.8430	1.4171	1.5000	1.7932	1.8007	2.2530	2.3670	2.5000	2.7262
F-SS1-F-SS1	FEMI	0.7076	1.0023	1.3578	1.7092	1.7687	1.8388	2.0184	2.1464	2.7000	2.7282
	FEMII	0.7049	1.0005	1.3571	1.6913	1.7661	1.8352	2.0042	2.1345	2.6713	2.6874
	Present	0.7041	1.0000	1.3569	1.6861	1.7653	1.8341	2.0000	2.1311	2.6546	2.6838
SS2-SS1-F-SS1	FEMI	1.0023	1.0675	1.4185	1.7851	1.8652	2.0184	2.3060	2.5866	2.8033	2.8419
	FEMII	1.0005	1.0660	1.4178	1.7822	1.8499	2.0042	2.2953	2.5776	2.7501	2.8364
	Present	1.0000	1.0655	1.4176	1.7815	1.8455	2.0000	2.2921	2.5752	2.7346	2.8353
C-SS1-F-SS1	FEMI	0.5003	1.1562	1.4604	1.5081	1.8848	2.1297	2.5373	2.6105	2.6670	2.8069
	FEMII	0.5001	1.1543	1.4596	1.5018	1.8694	2.1238	2.5084	2.5920	2.6586	2.7539
	Present	0.5000	1.1537	1.4594	1.5000	1.8649	2.1221	2.5000	2.5866	2.6564	2.7383
C-SS1-SS2-SS1	FEMI	0.5003	1.4304	1.5081	1.8182	2.3972	2.3975	2.5373	2.7886	2.8652	3.1606
	FEMII	0.5001	1.4295	1.5018	1.8140	2.3867	2.3928	2.5084	2.7650	2.8582	3.1455
	Present	0.5000	1.4293	1.5000	1.8128	2.3839	2.3913	2.5000	2.7582	2.8566	3.1414

and exact solutions will be implemented based on the established model in Section 2. Firstly, the effects of the boundary springs on fundamental frequency parameters of E-SS1-E-SS1, E-SS2-E-SS2, SS1-E-SS1-E, and SS2-E-SS2-E orthotropic rectangular plates are presented in Figures 6–9, respectively. For simplicity, every time only one type of boundary springs changes from 10^{-2} to 10^{16} uniformly and the resting springs keep infinity. The plate is characterized by $L_x = 1$ m and $L_y = 1.2$ m. From Figures 6–9, it can be found that different spring parameters have different effects on the vibration characteristics of the orthotropic rectangular plates. For the convenience of expression, two different types of elastic stiffness coefficients are represented by unified symbols k_n and k_p. It must be noted here that the symbols k_n and k_p represent the spring stiffness in the normal and parallel directions, respectively. For examples of E-SS1-E-SS1 and E-SS2-E-SS2, k_n is equivalent to k^u_{x0} and k^u_{x1} and k_p is equivalent to k^v_{x0} and k^v_{x1}. Similarly, for SS1-E-SS1-E and SS2-E-SS2-E, k_n is equivalent to k^v_{y0} and k^v_{y1} and k_p is equivalent to k^u_{y0} and k^u_{y1}. For the elastic parameters k_n and k_p, the influence of spring k_p on in-plane vibration characteristics is more severe. In addition, it can be found that regardless of the type of spring, when the spring stiffness coefficient is less than 10^5, the change of spring stiffness coefficient has little effect on the in-plane vibration characteristics of orthotropic rectangular plates in this region, while when the stiffness coefficient is between 10^5 and 10^{11}, the influence of spring stiffness coefficient variation on in-plane vibration characteristics of orthotropic rectangular plates is very severe in this region. When the stiffness coefficient exceeds 10^{11}, the change of spring stiffness coefficient has little effect on the in-plane vibration characteristics of orthotropic rectangular plates, so it can be considered as a clamped boundary condition. Based on this analysis, three types of elastic boundary restraints are defined and used in next calculation: E1: $k_n = k_p = 10^6$ N/m^2, E2: $k_n = k_p = 10^8$ N/m^2, and E3: $k_n = k_p = 10^{10}$ N/m^2.

Some new results of orthotropic rectangular plates with different elastically restrained edges are also performed in Tables 6–9. The geometrical dimensions of the plate are the

Table 3: Comparison of the in-plane frequency parameters Ω for E-SS2-E-SS2 orthotropic rectangular plates.

B.C	Method	Mode sequence									
		1	2	3	4	5	6	7	8	9	10
C-SS2-SS1-SS2	FEMI	1.0001	1.2699	1.7631	2.1352	2.2957	2.6989	3.0035	3.1312	3.1313	3.1598
	FEMII	1.0000	1.2684	1.7611	2.1228	2.2834	2.6887	3.0005	3.0868	3.1204	3.1286
	Present	1.0000	1.2679	1.7605	2.1192	2.2800	2.6859	3.0000	3.0735	3.1176	3.1190
C-SS2-C-SS2	FEMI	1.6926	2.0011	2.0025	2.5518	2.6157	2.8675	3.2100	3.3879	3.5414	3.6694
	FEMII	1.6908	1.9961	2.0002	2.5394	2.6063	2.8603	3.1651	3.3485	3.5254	3.6351
	Present	1.6904	1.9942	1.9999	2.5358	2.6037	2.8585	3.1524	3.3368	3.5209	3.6256
SS1-SS2-SS1-SS2	FEMI	1.0023	1.4558	2.0011	2.0184	2.2834	2.3052	2.4283	2.9241	3.0618	3.2465
	FEMII	1.0005	1.4541	2.0002	2.0042	2.2701	2.2963	2.4266	2.9109	3.0142	3.1983
	Present	1.0000	1.4537	2.0000	2.0000	2.2664	2.2937	2.4263	2.9073	3.0000	3.1847
SS1-SS2-F-SS2	FEMI	0.8458	1.4186	1.7974	1.8208	2.0011	2.2656	2.3757	2.7912	2.8190	2.8453
	FEMII	0.8436	1.4174	1.7942	1.8055	2.0002	2.2558	2.3689	2.7416	2.7961	2.8366
	Present	0.8430	1.4171	1.7932	1.8008	2.0000	2.2530	2.3670	2.7262	2.7895	2.8344
F-SS2-F-SS2	FEMI	0.7073	1.3578	1.7076	1.7687	1.8388	2.0011	2.1453	2.7000	2.7230	2.8419
	FEMII	0.7049	1.3571	1.6911	1.7660	1.8351	2.0002	2.1344	2.6707	2.6874	2.8364
	Present	0.7041	1.3569	1.6861	1.7653	1.8341	2.0000	2.1311	2.6546	2.6838	2.8342
SS2-SS2-F-SS2	FEMI	1.0001	1.0674	1.4185	1.7850	1.8638	2.3060	2.5861	2.7984	2.8419	3.0035
	FEMII	1.0000	1.0659	1.4178	1.7822	1.8498	2.2953	2.5776	2.7496	2.8364	3.0005
	Present	1.0000	1.0655	1.4176	1.7815	1.8455	2.2921	2.5752	2.7346	2.8353	3.0000
C-SS2-F-SS2	FEMI	1.0001	1.1561	1.4604	1.8834	2.1297	2.6104	2.6666	2.8021	3.0035	3.1088
	FEMII	1.0000	1.1543	1.4596	1.8692	2.1238	2.5920	2.6585	2.7533	3.0005	3.0970
	Present	1.0000	1.1537	1.4594	1.8649	2.1221	2.5866	2.6564	2.7383	3.0000	3.0940
C-SS2-SS2-SS2	FEMI	1.4304	1.8181	2.0011	2.3964	2.3975	2.7886	2.8651	3.1603	3.3149	3.5476
	FEMII	1.4295	1.8140	2.0002	2.3866	2.3928	2.7650	2.8582	3.1455	3.2773	3.5300
	Present	1.4293	1.8128	1.9999	2.3839	2.3913	2.7582	2.8566	3.1414	3.2664	3.5251

Table 4: Comparison of the in-plane frequency parameters Ω for SS1-E-SS1-E orthotropic rectangular plates.

B.C	Method	Mode sequence									
		1	2	3	4	5	6	7	8	9	10
SS1-SS1-SS1-C	FEMI	1.0025	1.1641	1.9226	2.0199	2.0969	2.3851	2.6221	2.8360	3.0669	3.1163
	FEMII	1.0005	1.1624	1.9187	2.0044	2.0821	2.3802	2.6089	2.8234	3.0148	3.0653
	Present	1.0000	1.1619	1.9177	2.0000	2.0779	2.3789	2.6052	2.8199	3.0000	3.0507
SS1-SS2-SS1-C	FEMI	0.5003	1.5081	1.5256	2.0834	2.3105	2.3576	2.5373	2.8240	2.9941	3.2595
	FEMII	0.5001	1.5018	1.5235	2.0818	2.2970	2.3511	2.5084	2.8100	2.9791	3.2112
	Present	0.5000	1.5000	1.5228	2.0815	2.2931	2.3493	2.5000	2.8060	2.9750	3.1974
SS1-C-SS1-C	FEMI	1.0025	1.6212	2.0199	2.1256	2.3417	2.8009	2.8713	3.0669	3.0676	3.2739
	FEMII	1.0005	1.6182	2.0044	2.1229	2.3277	2.7887	2.8564	3.0148	3.0504	3.2254
	Present	1.0000	1.6173	2.0000	2.1222	2.3237	2.7853	2.8522	3.0000	3.0457	3.2116
SS1-SS1-SS1-F	FEMI	0.5003	0.8989	1.4348	1.5081	1.8753	2.0745	2.2000	2.3506	2.5373	2.8321
	FEMII	0.5001	0.8965	1.4329	1.5018	1.8572	2.0725	2.1858	2.3436	2.5084	2.8074
	Present	0.5000	0.8957	1.4324	1.5000	1.8517	2.0720	2.1818	2.3417	2.5000	2.7894
SS1-C-SS1-F	FEMI	0.5003	1.0331	1.5081	1.8801	1.8982	2.2786	2.4362	2.5373	2.5754	2.8706
	FEMII	0.5001	1.0308	1.5018	1.8775	1.8801	2.2742	2.4297	2.5084	2.5616	2.8113
	Present	0.5000	1.0301	1.5000	1.8746	1.8768	2.2731	2.4279	2.5000	2.5577	2.7933
SS1-SS2-SS1-F	FEMI	1.0023	1.0089	1.8508	1.8951	2.0184	2.0199	2.3915	2.5217	2.8261	2.8702
	FEMII	1.0005	1.0068	1.8478	1.8771	2.0042	2.0185	2.3870	2.5088	2.8108	2.8130
	Present	1.0000	1.0061	1.8469	1.8716	2.0000	2.0182	2.3858	2.5052	2.7928	2.8094
SS1-F-SS1-F	FEMI	0.8097	1.0023	1.3993	1.8163	2.0159	2.0184	2.0341	2.1178	2.8084	2.8329
	FEMII	0.8068	1.0005	1.3971	1.7972	2.0042	2.0148	2.0173	2.1141	2.7726	2.7977
	Present	0.8059	1.0000	1.3965	1.7914	2.0000	2.0122	2.0146	2.1131	2.7544	2.7948
SS1-SS2-SS1-SS2	FEMI	1.0023	1.4558	2.0011	2.0184	2.2834	2.3052	2.4283	2.9241	3.0618	3.2465
	FEMII	1.0005	1.4541	2.0002	2.0042	2.2701	2.2963	2.4266	2.9109	3.0142	3.1983
	Present	1.0000	1.4537	2.0000	2.0000	2.2664	2.2937	2.4263	2.9073	3.0000	3.1847

Table 5: Comparison of the in-plane frequency parameters Ω for SS2-E-SS2-E orthotropic rectangular plates.

B.C	Method	Mode sequence									
		1	2	3	4	5	6	7	8	9	10
SS2-SS1-SS2-C	Du et al.	0.7071	1.1619	1.9178	2.0779	2.1215	2.3790	—	—	—	—
	Liu et al.	0.7071	1.1619	1.9177	2.0779	2.1213	2.3789	2.6052	2.8200	3.0508	3.2789
	Present	0.7071	1.1619	1.9177	2.0779	2.1213	2.3789	2.6052	2.8199	3.0507	3.2789
SS2-SS2-SS2-C	Du et al.	1.4142	1.5229	2.0814	2.2933	2.3496	2.8066	—	—	—	—
	Liu et al.	1.4142	1.5228	2.0815	2.2932	2.3493	2.8060	2.8284	2.9750	3.1975	3.3472
	Present	1.4142	1.5228	2.0814	2.2931	2.3493	2.8060	2.8284	2.9750	3.1975	3.3472
SS2-C-SS2-C	Du et al.	1.4142	1.6174	2.1222	2.3239	2.7857	2.8294	—	—	—	—
	Liu et al.	1.4142	1.6173	2.1222	2.3238	2.7853	2.8284	2.8522	3.0457	3.2116	3.6866
	Present	1.4142	1.6173	2.1221	2.3237	2.7852	2.8284	2.8522	3.0456	3.2116	3.6865
SS2-SS1-SS2-F	Du et al.	0.8957	1.4142	1.4324	1.8511	2.0719	2.1817	—	—	—	—
	Liu et al.	0.8957	1.4142	1.4324	1.8517	2.0720	2.1818	2.3417	2.7893	2.8158	2.8284
	Present	0.8957	1.4142	1.4324	1.8517	2.0720	2.1818	2.3417	2.7894	2.8157	2.8284
SS2-C-SS2-F	Du et al.	0.7071	1.0300	1.8740	1.8768	2.1215	2.2732	—	—	—	—
	Liu et al.	0.7071	1.0301	1.8746	1.8768	2.1213	2.2731	2.4279	2.5577	2.7932	3.2339
	Present	0.7071	1.0301	1.8746	1.8768	2.1213	2.2731	2.4279	2.5577	2.7933	3.2338
SS2-SS2-SS2-F	Liu et al.	0.7071	1.0061	1.8469	1.8716	2.0182	2.1213	2.3858	2.5053	2.7927	2.8094
	Present	0.7071	1.0061	1.8469	1.8716	2.0182	2.1213	2.3858	2.5052	2.7928	2.8094
SS2-F-SS2-F	Liu et al.	0.8059	1.3965	1.4142	1.7914	2.0122	2.0146	2.1131	2.7543	2.7948	2.8253
	Present	0.8059	1.3965	1.4142	1.7914	2.0122	2.0145	2.1131	2.7544	2.7948	2.8252
SS2-SS2-SS2-SS2	Liu et al.	1.4142	1.4537	2.0000	2.2665	2.2937	2.4263	2.8284	2.9074	3.1847	3.2155
	Present	1.4142	1.4537	1.9999	2.2664	2.2937	2.4262	2.8284	2.9073	3.1847	3.2155
	Liu et al.*	1.1785	1.3338	1.9994	2.0000	2.1889	2.3031	2.3570	2.6677	2.7491	3.0554
	Present	1.1785	1.3338	1.9994	1.9999	2.1889	2.3030	2.3570	2.6676	2.7491	3.0554

*Note that $b/a = 1.2$.

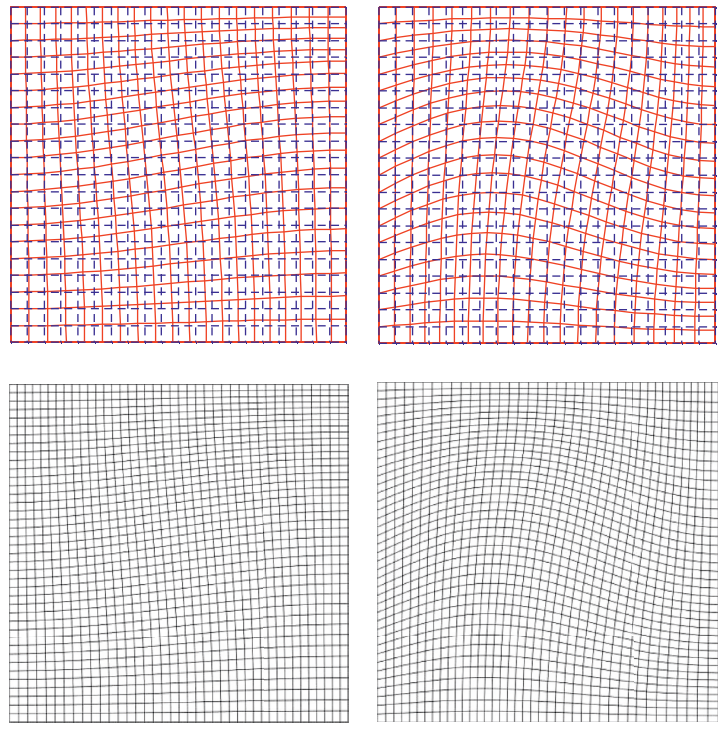

(a) (b)

Figure 4: Continued.

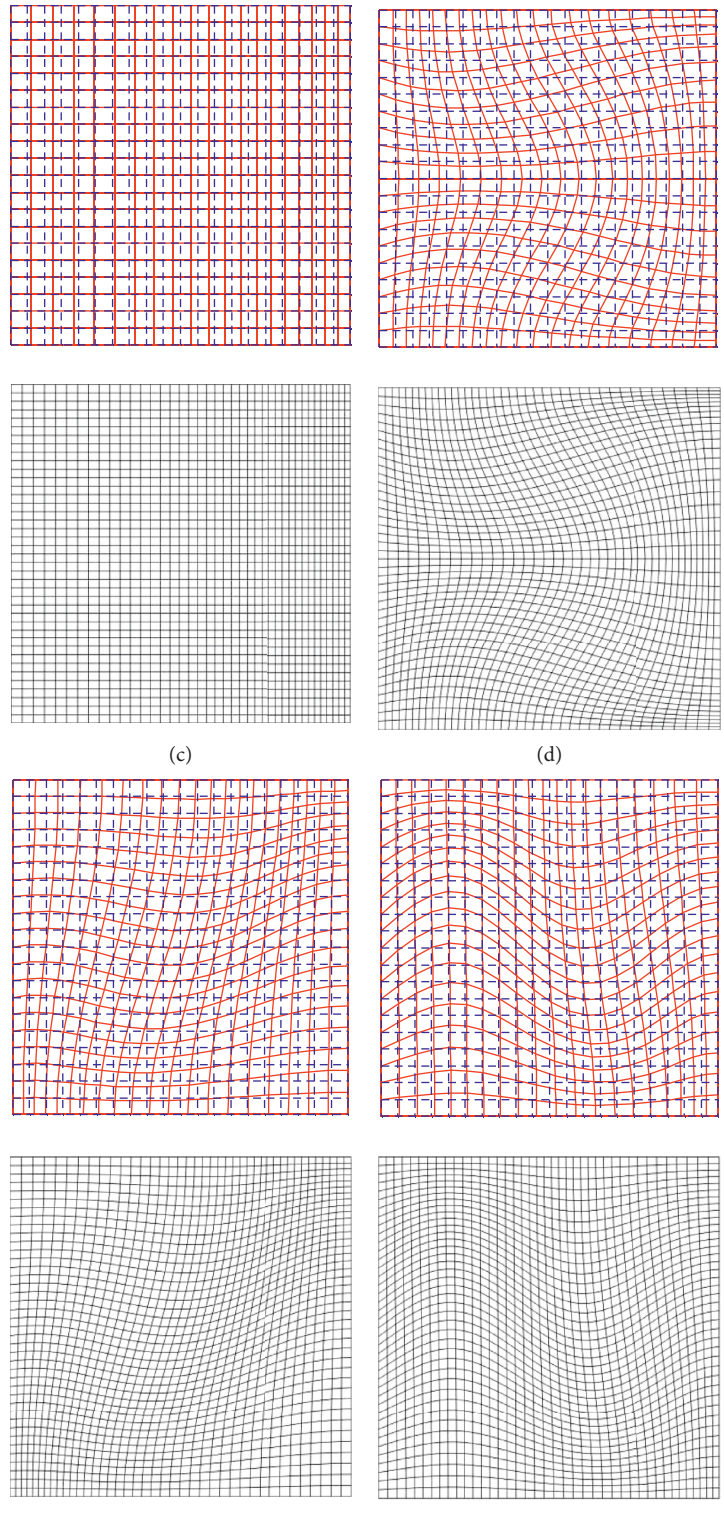

Figure 4: The mode shapes of the C-SS2-SS2-SS2 plate (red line: present solution; black line: ABAQUS software). (a) 1st mode. (b) 2nd mode. (c) 3rd mode. (d) 4th mode. (e) 5th mode. (f) 6th mode.

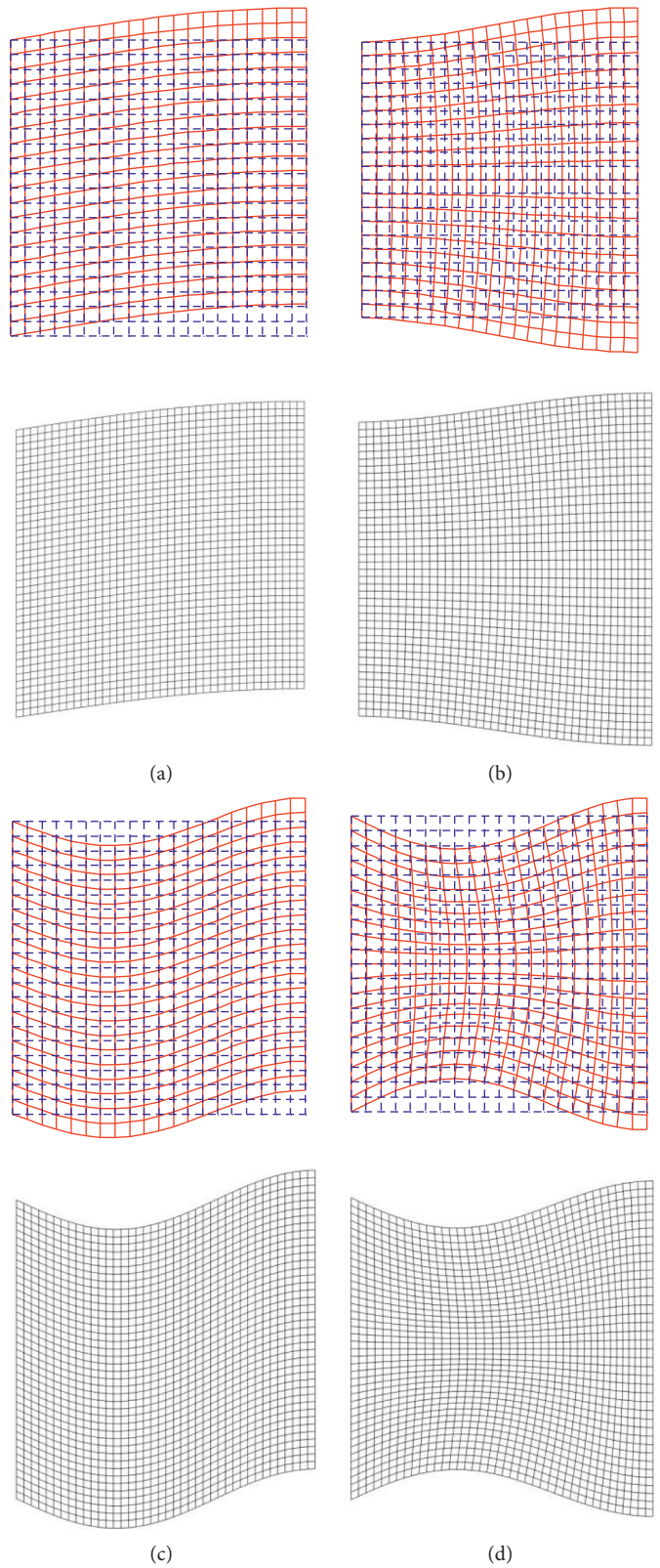

Figure 5: Continued.

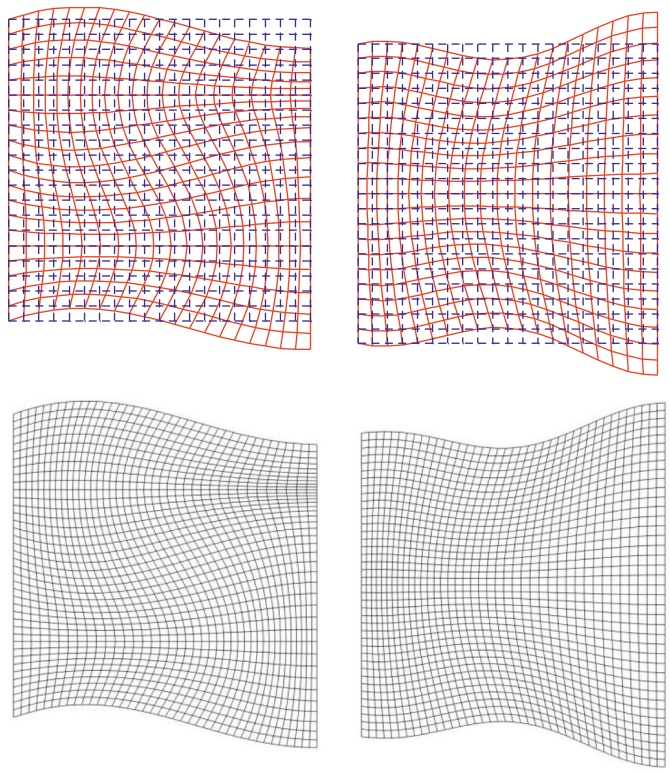

(e) (f)

Figure 5: The mode shapes of the C-SS1-SS2-SS1 plate (red line: present solution; black line: ABAQUS software). (a) 1st mode. (b) 2nd mode. (c) 3rd mode. (d) 4th mode. (e) 5th mode. (f) 6th mode.

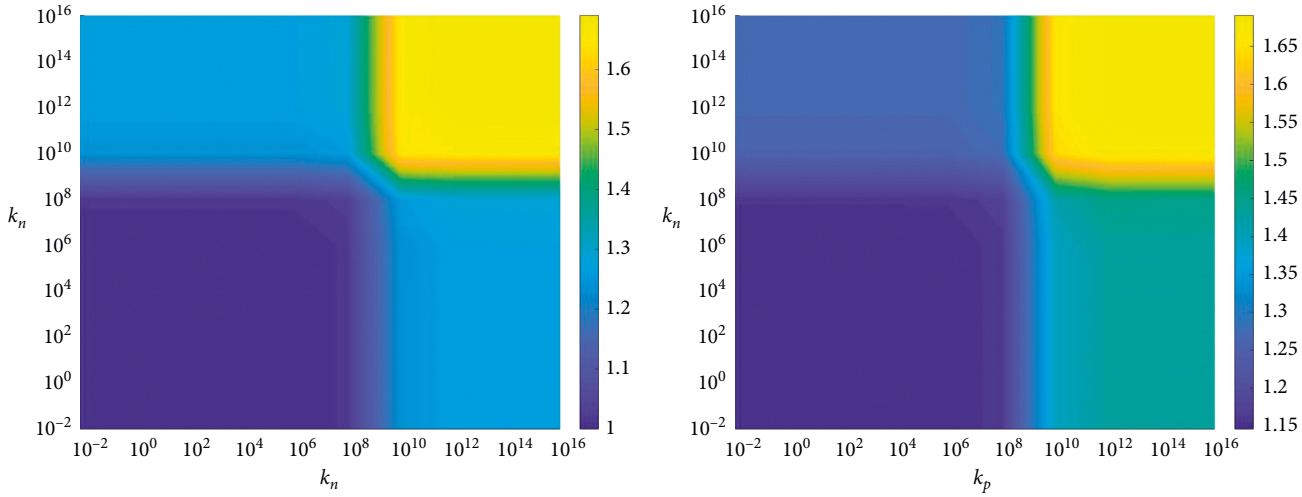

(a) (b)

Figure 6: Continued.

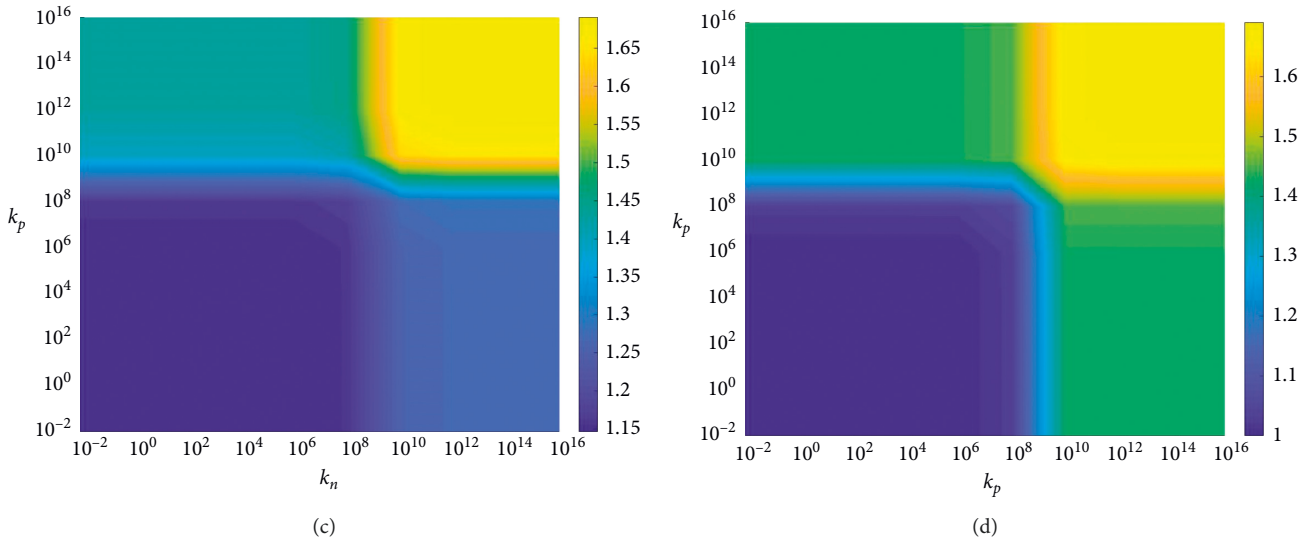

FIGURE 6: Effect of boundary spring stiffness on the fundamental frequency parameter of the orthotropic rectangular plate with E-SS1-E-SS1 boundary condition.

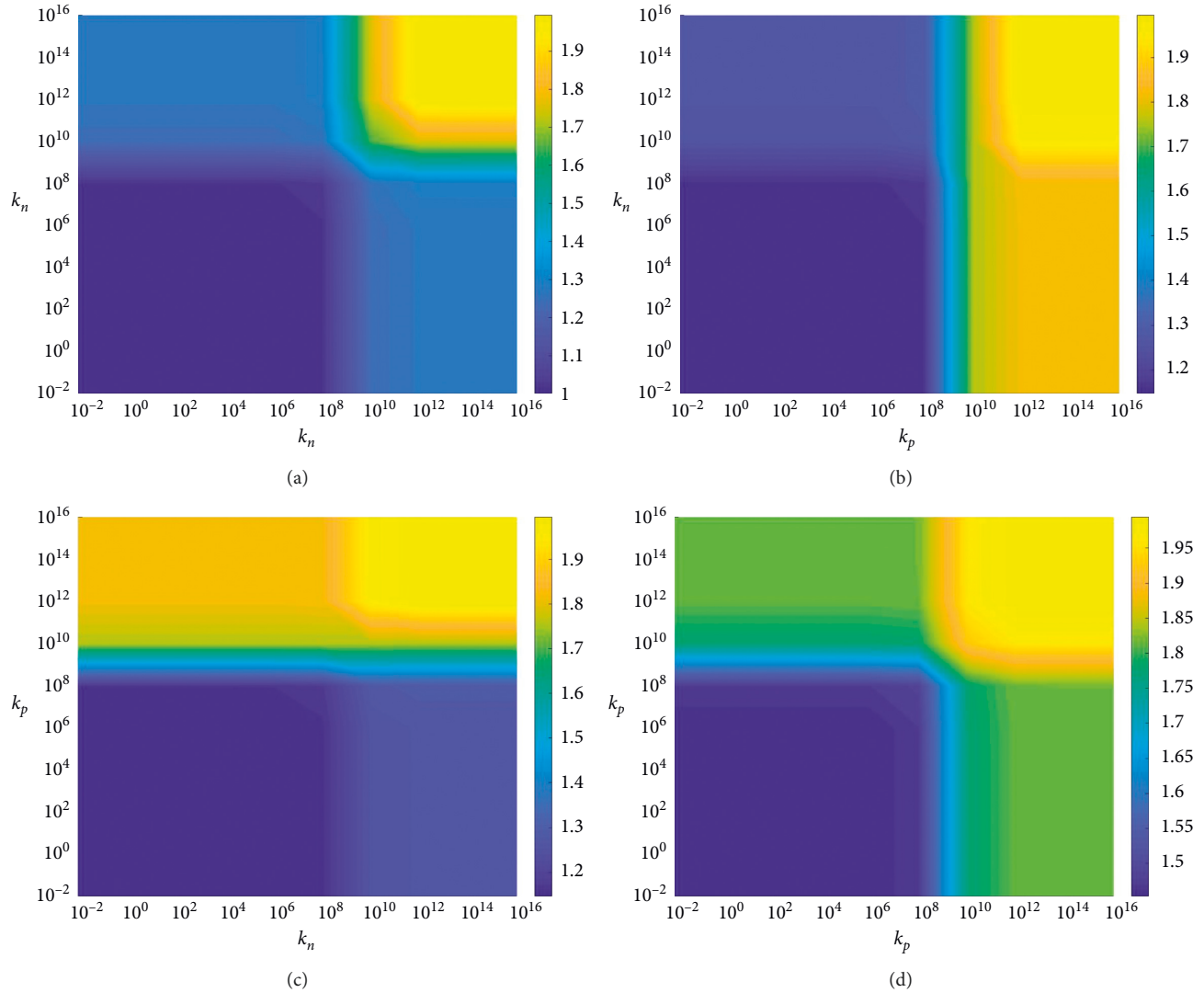

FIGURE 7: Effect of boundary spring stiffness on the fundamental frequency parameter of the orthotropic rectangular plate with E-SS2-E-SS2 boundary condition.

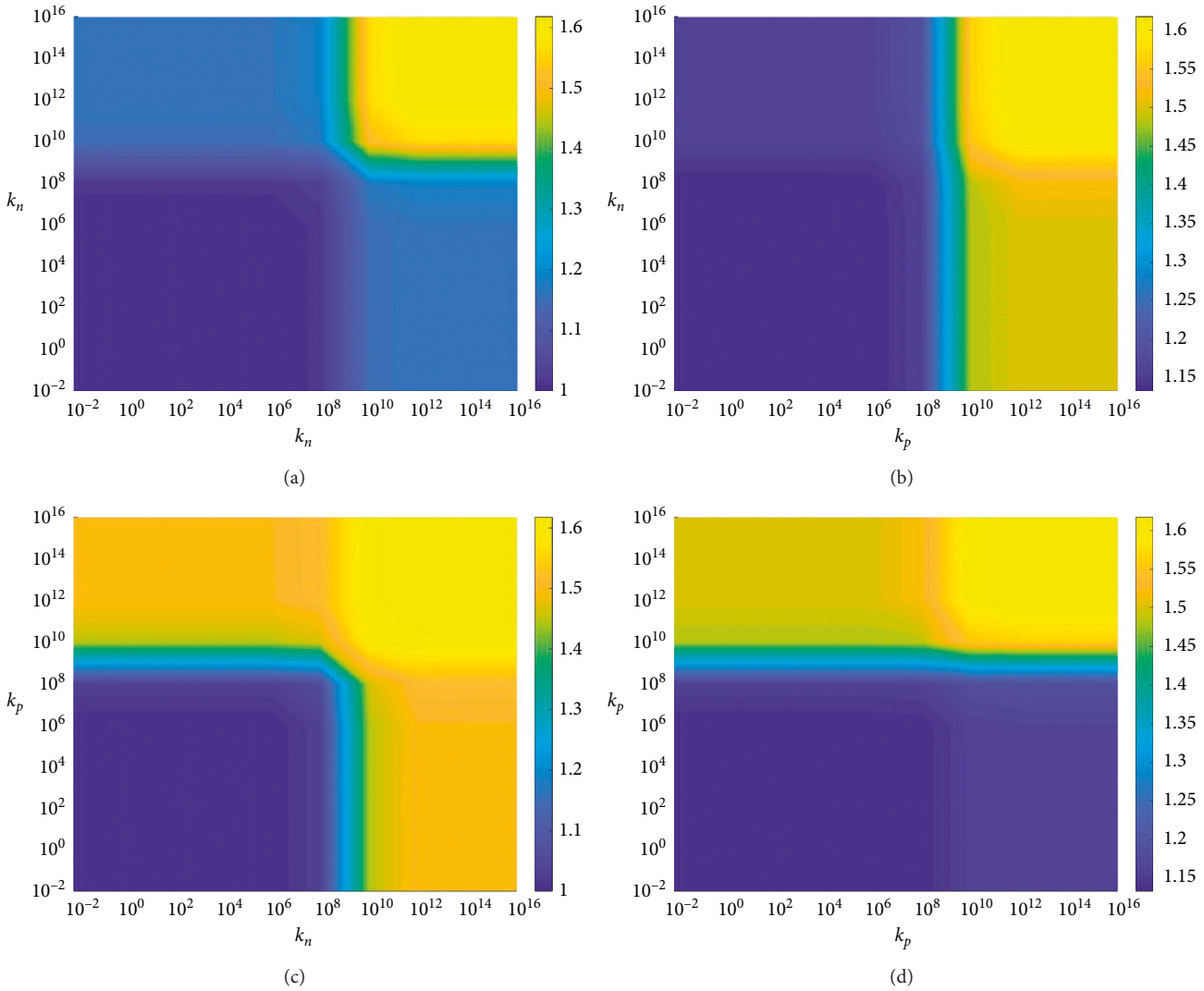

Figure 8: Effect of boundary spring stiffness on the fundamental frequency parameter of the orthotropic rectangular plate with SS1-E-SS1-E boundary condition.

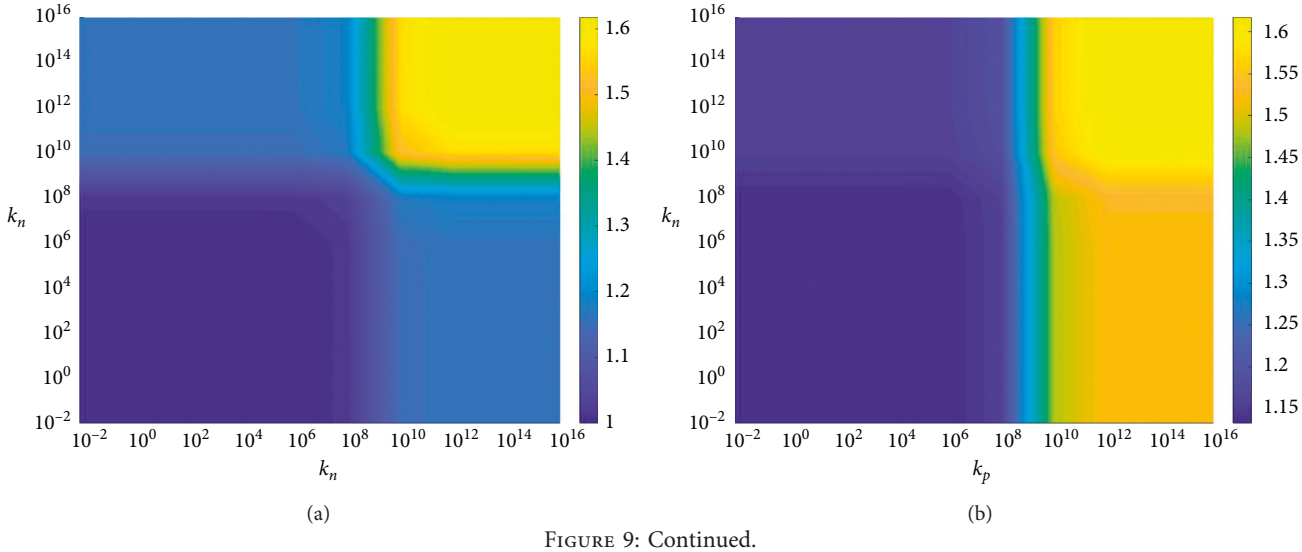

Figure 9: Continued.

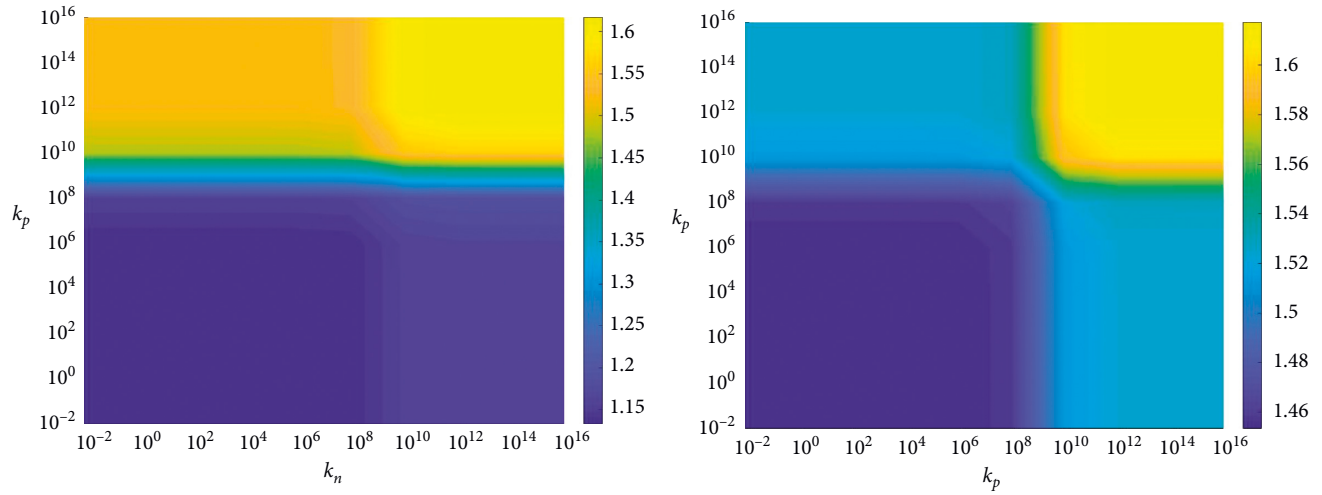

Figure 9: Effect of boundary spring stiffness on the fundamental frequency parameter of the orthotropic rectangular plate with SS2-E-SS2-E boundary condition.

Table 6: New in-plane frequency parameters Ω for E-SS1-E-SS1 orthotropic rectangular plates.

B.C	E_x/E_y	Mode sequence									
		1	2	3	4	5	6	7	8	9	10
E1-SS1-E1-SS1	2	0.0235	0.5455	1.0005	1.1406	1.3588	1.5891	1.8082	1.9324	2.0003	2.1735
	10	0.0239	0.5489	1.0006	1.1731	1.3637	1.6229	2.0003	2.1912	2.2785	2.3431
	20	0.0240	0.5493	1.0006	1.1760	1.3643	1.6266	2.0003	2.1929	2.3026	2.3511
	40	0.0240	0.5495	1.0006	1.1774	1.3646	1.6283	2.0003	2.1938	2.3126	2.3543
E2-SS1-E2-SS1	2	0.2299	0.6066	1.0524	1.1586	1.3893	1.6163	1.8462	1.9541	2.0273	2.1966
	10	0.2340	0.6140	1.0543	1.1951	1.3954	1.6508	2.0283	2.2128	2.3042	2.3524
	20	0.2345	0.6149	1.0545	1.1985	1.3961	1.6546	2.0284	2.2144	2.3275	2.3617
	40	0.2348	0.6154	1.0546	1.2001	1.3965	1.6564	2.0285	2.2152	2.3373	2.3654
E3-SS1-E3-SS1	2	0.9319	1.4491	1.6708	1.8653	2.1238	2.2206	2.3636	2.7831	2.8014	2.8881
	10	0.9342	1.4865	1.8698	2.1482	2.3384	2.4905	2.6391	2.8077	3.0096	3.0303
	20	0.9345	1.4939	1.8703	2.1868	2.4217	2.5103	2.7504	2.8085	3.0189	3.0388
	40	0.9347	1.4986	1.8706	2.1990	2.4771	2.5220	2.8089	2.8124	3.0233	3.0427

Table 7: New in-plane frequency parameters Ω for E-SS2-E-SS2 orthotropic rectangular plates.

B.C	E_x/E_y	Mode sequence									
		1	2	3	4	5	6	7	8	9	10
E1-SS2-E1-SS2	2	0.0235	0.5455	1.1405	1.3588	1.5891	1.8082	1.9324	2.0003	2.1735	2.3922
	10	0.0240	0.5489	1.1731	1.3637	1.6229	2.1912	2.2785	2.3430	2.6287	2.9453
	20	0.0240	0.5493	1.1760	1.3643	1.6266	2.1929	2.3026	2.3511	2.6398	3.0223
	40	0.0240	0.5495	1.1774	1.3646	1.6283	2.1938	2.3126	2.3543	2.6450	3.0241
E2-SS2-E2-SS2	2	0.2338	0.6066	1.1586	1.3893	1.6163	1.8462	1.9541	2.0273	2.1966	2.4158
	10	0.2393	0.6140	1.1951	1.3954	1.6508	2.2128	2.3042	2.3524	2.6437	2.9687
	20	0.2399	0.6149	1.1985	1.3961	1.6546	2.2144	2.3275	2.3617	2.6552	3.0387
	40	0.2403	0.6154	1.2001	1.3965	1.6564	2.2152	2.3373	2.3654	2.6606	3.0403
E3-SS2-E3-SS2	2	1.4491	1.5607	1.6708	2.1238	2.2206	2.3636	2.7831	2.8881	2.9160	3.1928
	10	1.4865	2.1464	2.1482	2.3384	2.4904	2.6391	3.0096	3.0303	3.2176	3.5750
	20	1.4939	2.1868	2.2674	2.4217	2.5103	2.7504	3.0189	3.0388	3.3094	3.6140
	40	1.4986	2.1990	2.3344	2.4771	2.5220	2.8124	3.0233	3.0427	3.3596	3.6348

same as those in Tables 6–9. The orthotropic ratios of the plate are $E_x/E_y = 2$, 10, 20, and 40. From Tables 6–9, it can be found that the frequency parameters of orthotropic rectangular plates increase gradually with the increase of orthotropic stiffness E_x/E_y, regardless of the boundary conditions. However, it is also obvious that when the

Table 8: New in-plane frequency parameters Ω for SS1-E-SS1-E orthotropic rectangular plates.

B.C	E_x/E_y	Mode sequence									
		1	2	3	4	5	6	7	8	9	10
SS1-E1-SS1-E1	2	0.0215	0.8339	0.8382	1.2395	1.6669	1.8157	1.9446	1.9534	2.0001	2.4507
	10	0.0219	0.8339	0.9355	1.4389	1.6669	1.9320	2.1911	2.4461	2.5002	2.9290
	20	0.0219	0.8339	0.9556	1.4762	1.6669	1.9550	2.2366	2.4946	2.5002	2.9564
	40	0.0219	0.8339	0.9695	1.4999	1.6669	1.9710	2.2670	2.5002	2.5209	2.9744
SS1-E2-SS1-E2	2	0.2090	0.8710	0.8852	1.2744	1.6938	1.8376	1.9681	1.9735	2.0155	2.4761
	10	0.2127	0.8870	0.9628	1.4728	1.6948	1.9474	2.2155	2.4648	2.5190	2.9407
	20	0.2131	0.8873	0.9817	1.5090	1.6950	1.9692	2.2597	2.5134	2.5191	2.9665
	40	0.2133	0.8874	0.9946	1.5319	1.6950	1.9842	2.2891	2.5191	2.5397	2.9835
SS1-E3-SS1-E3	2	0.7855	1.3654	1.5717	1.9086	2.1803	2.3593	2.3735	2.3995	2.6333	3.0425
	10	0.7871	1.4336	1.5749	2.2456	2.2847	2.3639	2.8616	3.1547	3.1677	3.2332
	20	0.7873	1.4433	1.5753	2.2532	2.3130	2.3645	2.8861	3.1554	3.1737	3.2927
	40	0.7874	1.4485	1.5755	2.2571	2.3270	2.3648	2.8987	3.1558	3.1768	3.3178

Table 9: New in-plane frequency parameters Ω for SS2-E-SS2-E orthotropic rectangular plates.

B.C	E_x/E_y	Mode sequence									
		1	2	3	4	5	6	7	8	9	10
SS2-E1-SS2-E1	2	0.0215	0.8382	1.1789	1.2395	1.8157	1.9446	1.9534	2.0001	2.3572	2.4507
	10	0.0219	0.9355	1.1789	1.4389	1.9320	2.1910	2.3572	2.4461	2.9290	2.9567
	20	0.0219	0.9556	1.1789	1.4762	1.9550	2.2366	2.3572	2.4946	2.9564	3.0095
	40	0.0219	0.9695	1.1789	1.4999	1.9710	2.2670	2.3572	2.5209	2.9744	3.0416
SS2-E2-SS2-E2	2	0.2118	0.8710	1.2164	1.2744	1.8376	1.9681	1.9735	2.0154	2.3764	2.4761
	10	0.2156	0.9628	1.2177	1.4728	1.9474	2.2154	2.3771	2.4647	2.9407	2.9725
	20	0.2161	0.9817	1.2179	1.5090	1.9692	2.2597	2.3772	2.5134	2.9665	3.0253
	40	0.2163	0.9946	1.2180	1.5319	1.9842	2.2891	2.3773	2.5397	2.9835	3.0573
SS2-E3-SS2-E3	2	1.0513	1.3654	1.9086	2.1089	2.1803	2.3734	2.3995	2.6333	3.0424	3.1156
	10	1.0554	1.4336	2.1165	2.2456	2.2847	2.8616	3.1677	3.1876	3.2332	3.6277
	20	1.0559	1.4433	2.1174	2.2532	2.3130	2.8861	3.1737	3.1888	3.2927	3.6487
	40	1.0561	1.4485	2.1178	2.2571	2.3270	2.8987	3.1768	3.1894	3.3178	3.6596

orthotropic stiffness E_x/E_y value is small, its change has a great influence on the in-plane vibration characteristics of the orthotropic rectangular plates, such as the orthotropic stiffness E_x/E_y value changing from 2 to 10. When the stiffness value is large, its change has little effect on the in-plane vibration characteristics, such as the orthotropic stiffness E_x/E_y value changing from 20 to 40. Since the in-plane vibration analysis of orthotropic rectangular plates with elastically restrained edges is conducted for the first time, thus, the results in Tables 6–9 can provide the reference for future research on the titled problem.

4. Conclusions

Based on the method of reverberation ray matrix (MRRM) and improved golden section search (IGSS) algorithm, an accurate solution is proposed and free in-plane vibration of orthotropic rectangular plates subjected to various boundary conditions is studied. The boundary condition is defined as that a set of opposite edges are with one kind of simply supported boundary conditions, where the rest two edges are arbitrary boundary conditions. In the current framework, the boundary simulation technique is introduced, where two opposite plate edges are implemented by the general elastic restraints (E) and the other two edges are simply supported restraints (S) containing the simply supported boundary 1 (SS1) and simply supported boundary 2 (SS2) to accord with the accurate solutions. Thus, the accurate solution with arbitrary specified boundary conditions can be easily obtained. The present accurate solutions are validated by both mathematical proof and comparisons with FEM solutions. By comparing with the existing literature, the main academic contributions of this paper can be summarized as the following two points: (a) By contrast with the existing accurate solution methods like direct separation of variables, the present accurate method breaks the barrier that the existing accurate solutions are always restricted to classical boundary conditions and adapts to more widespread boundary conditions on the premise of guaranteeing the accuracy of calculation. (b) Based on the existing in-plane accurate calculation results of orthotropic rectangular plates, some new in-plane accurate results are presented in this paper, which further enriches the solution system and calculation results of in-plane characteristics of orthotropic rectangular plates.

Data Availability

All the underlying data related to this article are available upon request.

Conflicts of Interest

The authors declare that there are no conflicts of interest regarding the publication of this paper.

Acknowledgments

The authors gratefully acknowledge the financial support from the National Natural Science Foundation of China (grant no. 51905511).

References

[1] R. Li, P. Wang, Z. Yang, J. Yang, and L. Tong, "On new analytic free vibration solutions of rectangular thin cantilever plates in the symplectic space," *Applied Mathematical Modelling*, vol. 53, pp. 310–318, 2018.

[2] R. Li, Y. Tian, P. Wang, Y. Shi, and B. Wang, "New analytic free vibration solutions of rectangular thin plates resting on multiple point supports," *International Journal of Mechanical Sciences*, vol. 110, pp. 53–61, 2016.

[3] R. Li, B. Wang, G. Li, and B. Tian, "Hamiltonian system-based analytic modeling of the free rectangular thin plates' free vibration," *Applied Mathematical Modelling*, vol. 40, no. 2, pp. 984–992, 2016.

[4] R. Li, X. Zheng, P. Wang et al., "New analytic free vibration solutions of orthotropic rectangular plates by a novel symplectic approach," *Acta Mechanica*, vol. 230, no. 9, 2019.

[5] S. Zhang and L. Xu, "Bending of rectangular orthotropic thin plates with rotationally restrained edges: a finite integral transform solution," *Applied Mathematical Modelling*, vol. 46, pp. 48–62, 2017.

[6] S. Zhang, L. Xu, and R. Li, "New exact series solutions for transverse vibration of rotationally-restrained orthotropic plates," *Applied Mathematical Modelling*, vol. 65, pp. 348–360, 2019.

[7] S. Ullah, Y. Zhong, and J. Zhang, "Analytical buckling solutions of rectangular thin plates by straightforward generalized integral transform method," *International Journal of Mechanical Sciences*, vol. 152, pp. 535–544, 2019.

[8] S. Ullah, H. Wang, X. Zheng, J. Zhang, Y. Zhong, and R. Li, "New analytic buckling solutions of moderately thick clamped rectangular plates by a straightforward finite integral transform method," *Archive of Applied Mechanics*, vol. 89, no. 9, pp. 1885–1897, 2019.

[9] N. S. Bardell, R. S. Langley, and J. M. Dunsdon, "On the free in-plane vibration of isotropic rectangular plates," *Journal of Sound and Vibration*, vol. 191, no. 3, pp. 459–467, 1996.

[10] A. N. Bercin and R. S. Langley, "Application of the dynamic stiffness technique to the in-plane vibrations of plate structures," *Computers and Structures*, vol. 59, no. 5, pp. 869–875, 1996.

[11] G. Wang, S. Veeramani, and N. M. Wereley, "Analysis of sandwich plates with isotropic face plates and a viscoelastic core," *Journal of Vibration and Acoustics*, vol. 122, no. 3, pp. 305–312, 2000.

[12] J. Du, W. L. Li, G. Jin, T. Yang, and Z. Liu, "An analytical method for the in-plane vibration analysis of rectangular plates with elastically restrained edges," *Journal of Sound and Vibration*, vol. 306, no. 3–5, pp. 908–927, 2007.

[13] D. Shi, Q. Wang, X. Shi, and F. Pang, "A series solution for the in-plane vibration analysis of orthotropic rectangular plates with non-uniform elastic boundary constraints and internal line supports," *Archive of Applied Mechanics*, vol. 85, no. 1, pp. 51–73, 2015.

[14] Y. F. Xing and B. Liu, "Exact solutions for the free in-plane vibrations of rectangular plates," *International Journal of Mechanical Sciences*, vol. 51, no. 3, pp. 246–255, 2009.

[15] N. H. Farag and J. Pan, "Free and forced in-plane vibration of rectangular plates," *The Journal of the Acoustical Society of America*, vol. 103, no. 1, pp. 408–413, 1998.

[16] Y. Chen, G. Jin, and Z. Liu, "Flexural and in-plane vibration analysis of elastically restrained thin rectangular plate with cutout using Chebyshev-Lagrangian method," *International Journal of Mechanical Sciences*, vol. 89, no. 89, pp. 264–278, 2014.

[17] D. J. Gorman, "Free in-plane vibration analysis of rectangular plates by the method of superposition," *Journal of Sound and Vibration*, vol. 272, no. 3–5, pp. 831–851, 2004.

[18] J. Seok, H. F. Tiersten, and H. A. Scarton, "Free vibrations of rectangular cantilever plates. Part 2: in-plane motion," *Journal of Sound and Vibration*, vol. 271, no. 1-2, pp. 147–158, 2004.

[19] L. Dozio, "Free in-plane vibration analysis of rectangular plates with arbitrary elastic boundaries," *Mechanics Research Communications*, vol. 37, no. 7, pp. 627–635, 2010.

[20] A. V. Singh and T. Muhammad, "Free in-plane vibration of isotropic non-rectangular plates," *Journal of Sound and Vibration*, vol. 273, no. 1-2, pp. 219–231, 2004.

[21] J. Du, Z. Liu, W. L. Li, X. Zhang, and W. Li, "Free in-plane vibration analysis of rectangular plates with elastically point-supported edges," *Journal of Vibration and Acoustics*, vol. 132, no. 3, pp. 1015-1016, 2015.

[22] M. Nefovska-Danilovic and M. Petronijevic, "In-plane free vibration and response analysis of isotropic rectangular plates using the dynamic stiffness method," *Computers and Structures*, vol. 152, pp. 82–95, 2015.

[23] D. J. Gorman, "Exact solutions for the free in-plane vibration of rectangular plates with two opposite edges simply supported," *Journal of Sound and Vibration*, vol. 294, no. 1-2, pp. 131–161, 2006.

[24] B. Liu and Y. Xing, "Exact solutions for free in-plane vibrations of rectangular plates," *Acta Mechanica Solida Sinica*, vol. 24, no. 6, pp. 556–567, 2011.

[25] Y. F. Xing and B. Liu, "Exact solutions for the free in-plane vibrations of rectangular plates," *International Journal of Mechanical Sciences*, vol. 51, no. 3, pp. 246–255, 2009.

[26] B. Liu and Y. Xing, "Comprehensive exact solutions for free in-plane vibrations of orthotropic rectangular plates," *European Journal of Mechanics-A/Solids*, vol. 30, no. 3, pp. 383–395, 2011.

[27] Y. Zhou, Q. Wang, D. Shi, Q. Liang, and Z. Zhang, "Exact solutions for the free in-plane vibrations of rectangular plates with arbitrary boundary conditions," *International Journal of Mechanical Sciences*, vol. 130, pp. 1–10, 2017.

[28] Y. Xue, G. Jin, X. Ma et al., "Free vibration analysis of porous plates with porosity distributions in the thickness and in-plane directions using isogeometric approach," *International Journal of Mechanical Sciences*, vol. 152, pp. 346–362, 2019.

[29] Z. Qin, X. Pang, B. Safaei, and F. Chu, "Free vibration analysis of rotating functionally graded CNT reinforced composite cylindrical shells with arbitrary boundary conditions," *Composite Structures*, vol. 220, pp. 847–860, 2019.

[30] M. Chen, G. Jin, T. Ye, and Y. Zhang, "An isogeometric finite element method for the in-plane vibration analysis of orthotropic quadrilateral plates with general boundary restraints," *International Journal of Mechanical Sciences*, vol. 133, pp. 846–862, 2017.

[31] H. Li, F. Pang, X. Miao, and Y. Li, "Jacobi-Ritz method for free vibration analysis of uniform and stepped circular cylindrical shells with arbitrary boundary conditions: a unified formulation," *Computers and Mathematics with Applications*, vol. 77, no. 2, pp. 427–440, 2019.

[32] H. Li, F. Pang, H. Chen, and Y. Du, "Vibration analysis of functionally graded porous cylindrical shell with arbitrary boundary restraints by using a semi analytical method," *Composites Part B: Engineering*, vol. 164, pp. 249–264, 2019.

[33] Z. Qin, Z. Yang, J. Zu, and F. Chu, "Free vibration analysis of rotating cylindrical shells coupled with moderately thick annular plates," *International Journal of Mechanical Sciences*, vol. 142-143, pp. 127–139, 2018.

[34] D. Shao, S. Hu, Q. Wang, and F. Pang, "Free vibration of refined higher-order shear deformation composite laminated beams with general boundary conditions," *Composites Part B: Engineering*, vol. 108, pp. 75–90, 2017.